MICROWAVE ECR PLASMA PROCESSING
of
THIN FILM SEMICONDUCTORS

by

The-Tu Chau

A thesis
presented to the University of Manitoba
in partial full fillment of the
requirements for the degree of
Master of Science
in
Electrical Engineering

Winnipeg, Manitoba, 1988

(c) The-Tu Chau, 1988.

Permission has been granted to the National Library of Canada to microfilm this thesis and to lend or sell copies of the film.

L'autorisation a été accordée à la Bibliothèque nationale du Canada de microfilmer cette thèse et de prêter ou de vendre des exemplaires du film.

The author (copyright owner) has reserved other publication rights, and neither the thesis nor extensive extracts from it may be printed or otherwise reproduced without his/her written permission.

L'auteur (titulaire du droit d'auteur) se réserve les autres droits de publication; ni la thèse ni de longs extraits de celle-ci ne doivent être imprimés ou autrement reproduits sans son autorisation écrite.

ISBN 0-315-44195-X

MICROWAVE ECR PLASMA PROCESSING OF
THIN FILM SEMICONDUCTORS

BY

THE-TU CHAU

A thesis submitted to the Faculty of Graduate Studies of
the University of Manitoba in partial fulfillment of the requirements
of the degree of

MASTER OF SCIENCE

© 1988

Permission has been granted to the LIBRARY OF THE UNIVERSITY OF MANITOBA to lend or sell copies of this thesis, to the NATIONAL LIBRARY OF CANADA to microfilm this thesis and to lend or sell copies of the film, and UNIVERSITY MICROFILMS to publish an abstract of this thesis.

The author reserves other publication rights, and neither the thesis nor extensive extracts from it may be printed or otherwise reproduced without the author's written permission.

ABSTRACT

Chemistry, physics and advanced technology play major roles in the transformation of silicon crystal wafers into advanced VLSI systems. One of the most interesting and important processing technologies is plasma processing. In this thesis some of the lastest microwave plasma processing systems are reviewed. Following this, results of the present study will be discussed, including; etching studies of Si and SiO_2 in a microwave electron resonance plasma (MECR), MECR plasma deposition of a-Si:H in the presence of an applied substrate potential, and the low-temperature MECR plasma deposition of insulating dielectrics. These studies have aided in our understanding of plasmas and plasma processing concerns of the microelectronics manufacturing industries. We have demonstrated that MECR systems present flexible alternatives which deserve further investigation, as they offer access to plasma processing conditions difficult to attain by any other means. It is quite reasonable to assume that MECR systems will become integral to the processing technology for material processing in the near future.

ACKNOWLEDGEMENTS

The author would like to acknowledge the valuable suggestion, assistance and guidance by Dr. McLeod throughout the whole course of this project. The author is also indebted to his colleagues at the Material and Devices Research Laboratory, in particular S.R. Mejia, T.V. Herak, J. Schellenberg, and P. Shufflebotham.

Financial support from the Natural Sciences and Engineering Research Council of Canada is gratefully acknowledged.

TABLE OF CONTENTS

	Page
ABSTRACT	ii
ACKNOWLEDGEMENTS	iii
INTRODUCTION	1
CHAPTER 1:Basic Plasmas and Their Application.	3
1.1 Nature of Plasmas.	3
1.2 Chemical Reactions in Plasmas.	4
1.3 Physics of Plasmas Etching.	5
1.4 Physical Chemistry of PECVD.	7
1.5 References for Chapter 1.	8
CHAPTER 2: ECR Microwave Systems Overview.	9
2.1 Introduction.	9
2.2 System 1: Hiroshima University.	11
2.3 System 2: Himeji Institute of Technology.	13
2.4 System 3: The Keizo Suzuki et.al System.	15
2.5 System 4: The Matsuo and Yoshio System.	17
2.6 System 5: The S.R. Mejia et.al System.	21
2.7 Conclusions.	23
2.8 References for Chapter 2.	24

CHAPTER 3: MECR Plasma Etching. 25
3.1 Introduction. 25
3.2 CF_4 Plasmas and the Role of Oxygen in Flourine Production. 26
3.3 Properties of Dry Etching. 30
3.4 Experimental. 31
3.4.1 Etch Rate versus Fluorine Concentration. 31
3.4.2 Etch Rate as a Function of Oxygen Concentration. 32
3.4.3 Power Dependence. 33
3.4.4 Pressure Dependence. 35
3.4.5 Magnetic Field Dependence. 37
3.5 Conclusions. 39
3.6 References for Chapter 3. 40

CHAPTER 4: a-Si:H Thin Film Deposition. 41
4.1 Introduction. 41
4.2 Experimental. 42
4.2.1 Substrate Potential, Deposition Rate versus Table Bias. 44
4.2.2 ε_2 and the Conductivity versus Table Bias. 47
4.3 Conclusions. 50
4.4.References for Chapter 4 51

CHAPTER 5: Silicon Oxide Deposition. 52
5.1 Introduction. 52
5.2 Experimental. 54
5.2.1 Deposition Rate versus Substrate Position. 55
5.2.2 FTIR Absorption Spectrum. 57
5.2.3 Thickness and Etch Rate. 61
5.3 Conclusions. 64
5.4 Future Trends. 64

5.5 References for Chapter 5. 65

CHAPTER 6: Conclusions. 66

TABLE OF FIGURES

		Page
[2.1]	MECR system developed at Hirishima University.	11
[2.2]	Plasma system developed at Himeji Institude of Technology.	13
[2.3]	Diagram of microwave plasma system built at Hitachi Limited.	15
[2.4]	The ECR system built at Musashino Electrical Communication Laboratory.	18
[2.5]	Modification of System 2.4.	19
[2.6]	ECR system developed at the University of Manitoba.	22
[3.1a]	OES Spectrum of CF_4 plasma in the absence of O_2.	28
[3.1b]	OES Spectrum of CF_4 plasma with 10% of oxygen added.	28
[3.2]	Etch rate and [F]/[O] ratio as a function of O_2 concentration.	33
[3.3]	Etch rate as a function of Power.	34
[3.4]	Very rough surface of Si after etching under high power Absorption.	35
[3.5]	Etch rate as a function of pressure.	36
[3.6]	Etch rate as a function of magnetic field and [F]/[O] ratio.	38
[4.1]	Modification Chamber for a-Si:H films growth study.	43
[4.2]	Difference between the plasma potential and the floating potential V_p - V_f and between the plasma potential and the table bias voltage V_p - V_b as function of V_b.	45
[4.3]	Deposition rate as functions of bias voltage.	46
[4.4]	ε_{2max} against table bias.	47
[4.5]	Dark conductivity and σ_{ph}/σ_d as a function of the table bias.	48

[5.1] Chamber modification for SiO_2 film growth. 54

[5.2] Deposition rate versus substrate position. 56

[5.3] IR absorption spectrum of an as-deposited film. 57

[5.4] γ_m and Δ_m versus substrate position. 58

[5.5] Film absorbance versus thickness. 59

[5.6] Change of IR spectrum after annealing. 60

[5.7] Change in the film thickness after annealing. 61

[5.8] Etching rate of as-deposited and annealed films as functions of substrate position. 63

INTRODUCTION

The continuing demand for inexpensive electronic circuits has created a rapidly growing microelectronic industry. The economic pressure for lower cost, lower power consumption and the functional need for higher operational speed have led to ever increasing levels of integration.

In the past, the process used in semiconductor integrated circuit fabrication was primarily wet etching and thermal processes such as oxidation, diffusion, and chemisorption. However, these processes posed many problems that could not be solved as the scale of the device dimension shrunk. Some of these problems are ; i) the wet etching process is isotropic, difficult to automate, with the waste difficult to handle and dispose of and, ii) thermal processes consume a considerable amount of energy, in addition they induce impurity diffusion, dislocation, and stacking faults in the semiconductor substrate. Furthermore, thermal process induces difficulty in multi-layer formation. On other hand, plasma processing of materials seem to have solved most of the conventional problems. For example, plasma etching can be anisotropic, and easy to automate. There are no serious problems in substrate handling or waste gas disposal. In addition, thin films can be deposited and doped at low temperature by low pressure plasma enhanced chemical deposition.

Although the plasma process has been widely studied and applied, the science and technology of dry processing continues to be recognized globally as a frontier area of research and development work. In this thesis, chapter 1 will review basic plasma

chemistry and some applications. Chapter 2 will describe some of microwave ECR plasma systems which are currently used in research and industry. Chapter 3 will present results of our etching studies of Si and SiO_2 using of CF_4 and O_2 in our microwave ECR system. Chapter 4 will present a study of biasing effects on a-Si:H films grown under SiH_4 and H_2 gaseous mixture. Chapter 5 presents the preliminary results of growing SiO_2 insulating films using O_2 and SiH_4. Finally, chapter 6 will briefly highlight some of the important results that we have observed during our course of study.

CHAPTER 1

Basic Plasmas and Their Application.

1.1 Nature of Plasmas.

A plasma, in general, is described as an neutral mixture of ions and electrons. The type of plasma used for the processing of semiconductor material is commonly referred to as glow discharge, where the additional energy supplied to sustain plasma is usually radio frequency (rf) electromagnetic radiation. Such plasmas are typically maintained at 10^{-2} to 1 torr and are characterized by a small degree of ionization which allows the plasma to be treated by the gas laws. Due to the thermal non-equilibrium between gas molecules and free electrons, it is possible to achieve electron temperatures on the order of 10^4 to 10^5 K (1 to 2 eV) while at the same time the gas temperature may be held at or near the ambient level (300 K).

The basic characteristics of plasmas involve electron temperature, electron density, and plasma frequency. The plasma frequency † is the natural oscillation frequency of the plasma due to its collective behavior. When the plasma is perturbed by any means, the plasma will react collectively to counter act that perturbation. To confine a plasma, a DC magnetic field is often introduced into the plasma. If the magnetic field is high enough, the plasma is strongly influenced by the interaction of the magnetic field and the electromagnetic excitation. The critical frequency is called the cyclotron frequency w_c [1]. When this condition is

† A more detailed explanation is given in Appendix A.

satisfied, the plasma appears very absorbing due to a natural resonance. The system power requirements are therefore greatly reduced. This condition is also known as Electron Cyclotron Resonance (ECR).

1.2 Chemical Reactions in Plasmas.

The reactions which occur in plasmas are usually quite complex. Normally, the reactions are initiated by collisions between energetic free electrons and gas molecules to form various reactive species. Collisions between electrons and gas molecules can be characterized as either elastic or inelastic. In the former case a very small fraction of the electron energy is transferred to the molecule. This results in an increase in the kinetic energy of the gas and hence the gas temperature. Inelastic collisions involve much larger electron energy losses and the excitation of internal modes of the target molecule. Depending upon the energy of the impacting electron, the molecule undergoing inelastic collision can be excited in the following ways [2].

Excitation

$$e + A_2 \rightarrow A_2^* + e$$

Dissociative Attachment

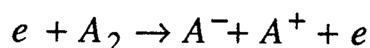

$$e + A_2 \rightarrow A^- + A^+ + e$$

Dissociation

$$e + A_2 \rightarrow 2A + e$$

Ionization

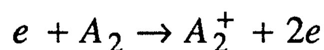

$$e + A_2 \rightarrow A_2^+ + 2e$$

Dissociative Ionization

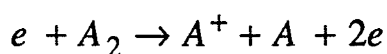

$$e + A_2 \rightarrow A^+ + A + 2e$$

In addition to excitation there is also a relaxation state which does not involve an electron collision, illustrated as follows.

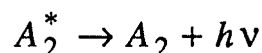

$$A_2^* \rightarrow A_2 + h\nu$$

The relaxation state is very useful in optical emission spectrography (OES) for plasma diagnostics. In addition, an individual emission line from the plasma can be monitored for control during etching or thin film deposition.

1.3 Physics of Plasma Etching.

Plasma etching is a process where gas is discharged in the plasma and reacts with a surface to remove material by forming gaseous product molecules. It is suggested that the reactive gas components from the plasma appear to be adsorbed on the surface. The products of the reaction with the absorbed layer and the surface are then desorbed as gaseous by-products and pumped away. In general, the process can be described as

$$A(g) + B(s) \rightarrow AB(g)$$

Because of its chemical nature, a high degree of control over the relative etch rates for various substrates can be obtained by the choice of suitable masking materials and feed stock gases.

For example one application is the stripping of photoresist in a low pressure oxygen rf glow discharge. Hardened photoresists

are required to be extremely inert polymers so as to resist etchants that may otherwise attack the substrate they cover. This same property makes them difficulty to remove by wet chemical processes or even organic solvents. However, when the polymer chains are oxidized in a glow discharge, the gaseous by-products are easily pumped away. This technique is generally used to removed carbonaceous contamination[2].

Glow discharge in low-pressure fluorocarbon (CF_4) vapors or mixtures of fluorocarbon with various additives gases (O_2 or H_2) are currently being used for patterning silicon, silicon dioxide, and other material used in IC fabrication. The chemically active radicals formed by the glow discharge react with silicon and its compounds to form gaseous SiF_4. For example,CF_4 is assumed to decomposed in to CF_3, CF_2, CF, and atomic fluoride [3].

$$CF_4 \rightarrow CF_3 + F$$

$$CF_4 \rightarrow CF_2 + 2F$$

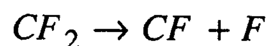

$$CF_2 \rightarrow CF + F$$

Reactions are then assumed to proceed as follow

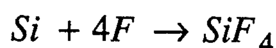

$$Si + 4F \rightarrow SiF_4$$

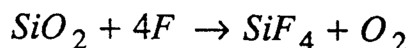

$$SiO_2 + 4F \rightarrow SiF_4 + O_2$$

Hence removing the solid Si or SiO_2.

Reactive plasma etching is currently being intensively studied. It is anticipated that many more applications and an understanding of the detailed mechanism involved will be forthcoming.

1.4 Physical Chemistry of PECVD.

Chemical vapor deposition (CVD) is a surface reaction in which a gas or gases react with a surface at high temperature, usually at about 1 atm. Plasma enhanced CVD (PECVD) is a process in which a plasma activates a gas or gases which may react with a surface at a relative low temperature. For example, CVD and PECVD of silicon oxide films are expressed as:

CVD

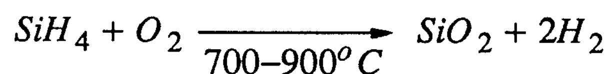

$$SiH_4 + O_2 \xrightarrow[700\text{–}900^oC]{} SiO_2 + 2H_2$$

PECVD

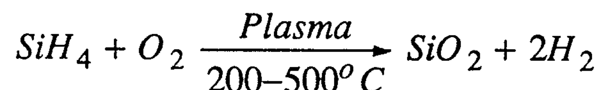

$$SiH_4 + O_2 \xrightarrow[200\text{–}500^oC]{Plasma} SiO_2 + 2H_2$$

In the present studies, PECVD is widely used in the formation of several thin films. With the use of a plasma, the temperature of the substrate can be lowered and thermal damage of the film reduced. The reason why the temperature of the substrate can be lowered may be explained as follows. In the plasma, the energy of the electrons is larger than that of the ions or neutrals particles (thermal non-equilibrium state). Although the energy of the ions and neutral particles are relative low, these particles become excited by colliding with electrons. This excited state is equivalent to a high-temperature induced activation, and the effective reaction can thus proceed at a low-temperature. Various states of the species in the plasma depend on how the plasma was generated, pressure, and other parameters.

1.5 References for Chapter 1

1 A. Arzimovich, *Elementary Plasma Physics,* Blaisdell publishing Company, New York, 1965.

2 T.T. Chau, *B.Sc. Thesis,* University of Manitoba, Dept. of Electrical Engineering, pp. 10-12, 1986.

3 I. Brodie and J.J. Muray, *The Physics of Microfabrication,* Plenum Press, New York, pp. 294-250, 1982.

CHAPTER 2

ECR Microwave Systems Overview.

2.1 Introduction.

Radio frequency (rf) plasma processing of semiconductor materials has become an established industrial technique, while microwave induced plasma (MIP) processing of materials has only recently begun to be explored. The MIP can be operated at pressures ranging from as low as 10^{-4} torr to above atmospheric pressure and at powers from 4 Watts to about 400 Watts [4, 5]. The MIP can be contained in a vacuum sealed electrodeless discharge chamber [1, 2] or can be operated as flowing continuous systems [4, 5]. The equipment needs for MIP generation is relatively simple, consisting of only a plasma containment tube, a microwave generator, and a component (coupling device or antenna) which facilities transfer of energy from the power supply to the plasma.

In this chapter, we review system apparatus for plasma enhanced chemical vapor deposition (PECVD) and plasma enhanced chemical etching (PECE) processing in semiconductor technology. In lieu of describing all of rf, microwave, and microwave ECR plasma systems, we only focus on microwave ECR (MECR) plasma system configurations and their application in industry and research. MECR systems designed by several Japanese laboratories are first reviewed and discussed. The

chapter also will briefly describe the MECR plasma system which was developed at the Department of Electrical Engineering of the University of Manitoba. Although all the systems are only at the research stage, some of them are good candidates for adoption in industry as substitutes for rf plasma processing. Ion sources can also be built using MECR plasma systems [9] and represent addition application areas for MECR plasmas with great potential.

2.2 System 1: Hiroshima University.

The first MECR system that we chose to review was made at Hiroschima University [1]. The configuration for this system is very simple. Figure 2.1 shows the schematic representation of the system.

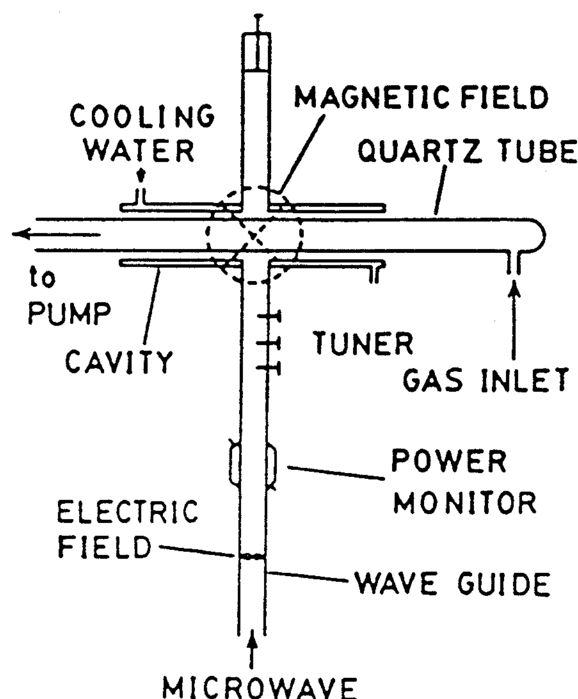

Figure 2.1: *MECR system developed at Hiroshima University.*

The ECR plasma was formed in the quartz tube inserted in the cylindrical cavity. Microwave power was fed in the TE_{10} mode, at a frequency of 2.45 GHz. A magnetic field (875 G at the ECR condition) perpendicular to the electric field was applied

external to the cavity. Substrates were laid at the center of the cavity. The substrate temperature was monitored by means of an infrared thermometer (900 nm wavelength).

This system has been used to study SiC films fabrication in the gas mixture of SiH_4, CH_4, and H_2 [1]. The authors recorded that the power and pressure had effected the crystalline grain size. However, the deposition rate was uneffected with respected to pressure change. When reviewing this system, severals points were noted; i) The minimum microwave power used is 80 Watts; ii) The operating pressure is between 2 - 10 torr (very high pressure for MECR systems); iii) Microwave radiation is expected to leak to the environment, hence it is a hazard to the health of the operator; and iv) The substrate is inherently heated by microwave radiation. Hence cooling is needed to cool down the substrate if one wants to study low-temperature thin film processing.

2.3. System 2: Himeji Institute of Technology.

This system is similar to the previous system in the manner that the plasma is generated. Figure 2.2 shows the schematic of the plasma system. The quartz tube is modified to become a quartz chamber. The microwave frequency used is 2.45 GHz and the coaxial magnet surrounding the quartz chamber has a flux density of approximately 270 G. As such, the ECR condition is not reached, but the magnetic field still acts to confine the plasma [2].

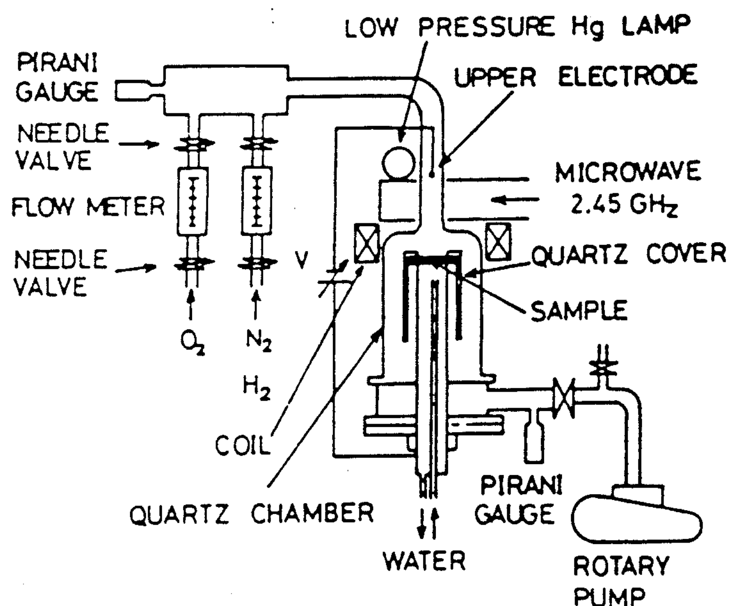

Figure 2.2: *Plasma system developed at Himeji Institute of Technology.*

Tetsuro Matsuda et.al have used this system to study the oxidation of Si by an oxygen plasma through protective aluminum coatings. There is no information of film deposition or etching for this system yet. However, the research on oxidation of Si has contributed some interesting ideas in combining microwave and photo assisted plasmas for material processing. As with the previous system, there are still some disadvantages such as substrate self heating, high microwave power consumption, and microwave radiation leakage.

2.4. System 3: The Keizo Suzuki et.al system.

The Suzuki system was developed at Central Research Laboratory of Hitachi Limited, Kokubunji, Tokyo. Figure 2.3 shows the system configuration [3]. An air cooled, 60 mm inside diameter, round discharge tube is inserted at the termination end of a round waveguide. The microwave frequency is 2.45 GHz, the microwaves propagate to the discharge area through rectangular and round waveguide sections. Two coils and a permanent magnet are used to produce a mirror type magnetic field in the discharge area, which confines the plasma effectively. The maximum and the minimum magnetic flux density are 2100 G and 500 G respectively.

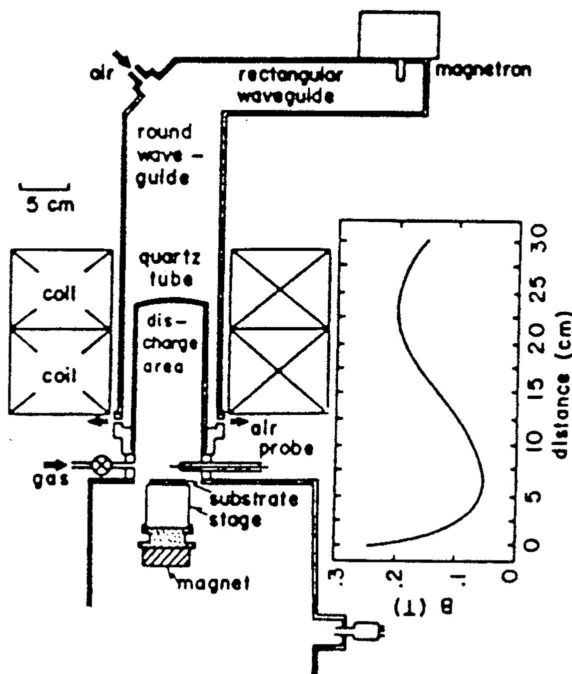

Figure 2.3: *Diagram of microwave plasma system built at Hitachi Limited.*

The plasma density and electron temperature can be calculated from measurements with a cylindrical single probe placed between the substrate and the discharge area. The probe was made of tungsten wire, 0.27 mm in diameter and 2.3 mm long. In general, interpretation of probe data is still an area of considerable research efforts.

This system has been used to study etching of Si and SiO_2 as functions of pressure and gas mixture. The authors recorded that this system yields a high plasma density ($n_p = 1 - 7 \times 10^{11}\ cm^{-3}$) and low electron temperature ($kT_e \approx$ 3-5 eV) at a microwave power of 180 Watt and pressure of 10^{-3} torr. The etching mechanism of Si and SiO_2 in $CF_4 + O_2$ plasmas tend to be anisotropic at reduced pressure (typically below 10^{-4} torr). The etch rate and selectivity are dependent upon the CF_4 and O_2 mixture in the manner similar to rf systems, in spite of the lower pressures.

The Suzuki system was a good contribution to MECR plasma system design. The system and method can be adapted to semiconductor processing in a production environment.

2.5. System 4: The Matsuo and Yoshio System.

The Matsuo system [4] was developed at Musashino Electrical Communication Laboratory, Nippon Telegraph and Telephone Public Corporation, Musashino - Shi - Tokyo 180. Figure 2.4 illustrates the system apparatus. The microwave power (at 2.45 GHz) is fed into the discharge chamber by a rectangular waveguide and through a window made of fused quartz [4]. The discharge chamber is 20 cm in diameter and 20 cm in height, and operates as a microwave cavity resonator in the TE_{113} mode. Magnetic coils are arranged around the periphery of the discharge chamber to achieve the ECR condition. The ion extraction system, produces a 15 cm board beam, and is composed of two stainless steel grids 1 mm apart with aligned multiple holes 2 mm in diameter. The upper grid makes electrical contact with the discharge chamber, and the lower grid is at ground potential. The ion attraction voltage (0 - 1000 V) is applied to the whole discharge chamber. The discharge chamber and the magnetic coils are water cooled. The vacuum system consists of an oil diffusion pump (1200 $\frac{l}{s}$) and a mechanical rotary pump (500 $\frac{l}{\min}$). Gases were introduced through inlet (1) and inlet (2).

If the intensity of the magnetic field in the discharge chamber is gradually reduced from the ECR condition at the top toward the attraction grids, this magnetic field serves to improve the intensity of the extracted ion current and the uniformity of the current density. In effect, the ions are transported along the divergent magnetic field and are spread more uniformly over the grids.

The ion current density can be monitored by a Faraday cup attached to a shutter plate at the substrate table.

The system operates between 100 - 300 Watts of input microwave power. Etching of Si, SiO_2 and Al as a functions of ion attraction voltage was reported. The pressure was maintained at 0.3×10^{-5} torr. High etch rates of Si (400 Å/sec), SiO_2 (200 Å/sec), and Al (1500 Å/sec) had been recorded at 1000 V attraction voltage.

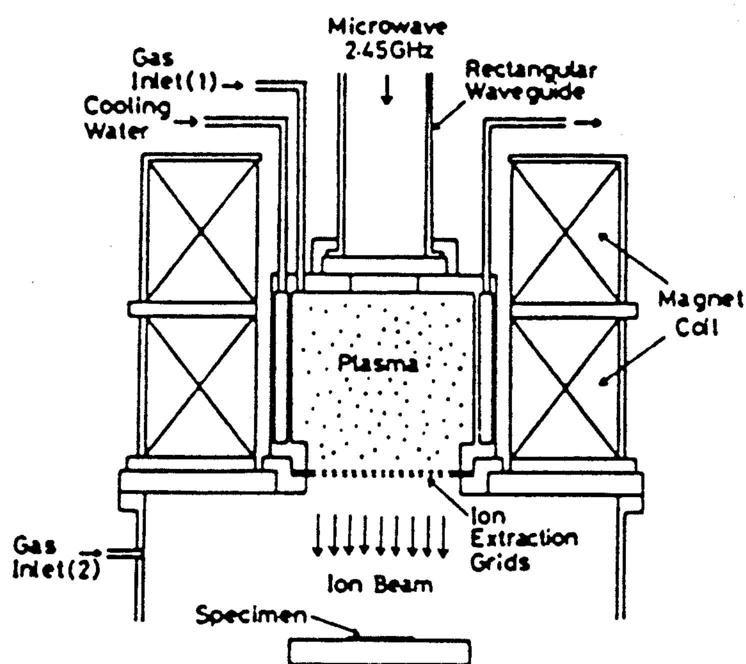

Figure 2.4: *The ECR system built at Musashino Electrical Communication Laboratory.*

The same system configuration without the bias voltage, was also used to study thin film deposition of SiO_2, a-Si:H, and Si_3N_4. The deposition of insulating thin films such as Si_3N_4 and SiO_2 were recorded at low temperature (250 - 350°C) and low pressure (10^{-4} torr). The physical properties of those films showed that they are comparable to the high temperature CVD and the thermal oxidation. At the present time electrical data is unavailable.

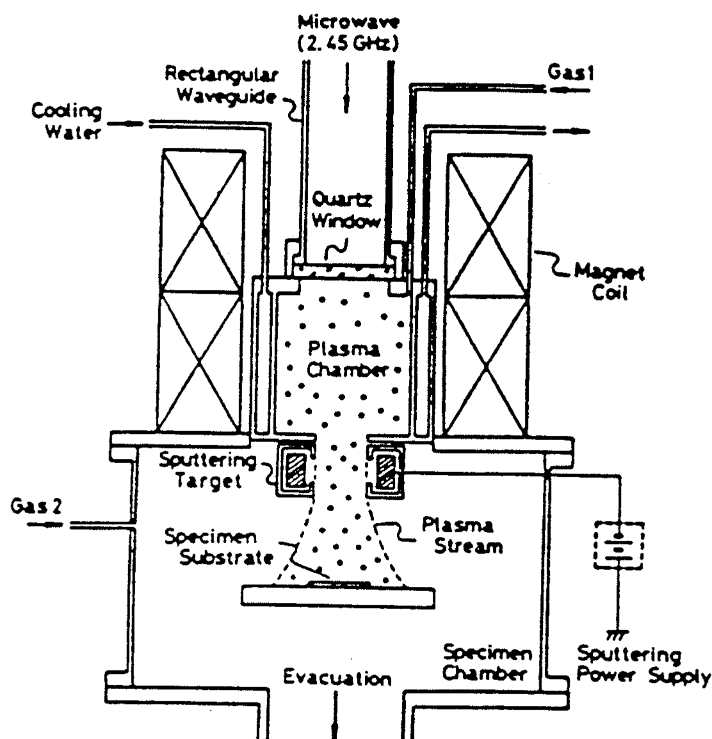

Figure 2.5: *Modification of System 2.4.*

With the same basic system configuration, Tono et.al had modified the ECR plasma technique for metal and metallic

compound deposition [5]. Figure 2.5 shows the new version of system 4. A DC voltage is supplied to the target placed around the extracted plasma stream. The target substrate is indirectly cooled by water. The sputtering gas (Ar) was introduced into the plasma chamber while the reaction gas (O_2) was introduced into specimen chamber. The sputtering occurred with ions from the plasma stream. Sputtered particles were ionized by collisions with electrons in the plasma stream and were transported to the specimen substrate by the self generated electric field and by the effect of divergent magnetic field. Because of high ionization and subsequent ion bombardment of the targets, metal and metallic compound films of high quality can be obtained with high efficiency and without the need for substrate heating. Films of tantalum, tantalum oxide, Al, AlO_2 were deposited by this system. Full details of the studies are given in reference [5,6].

In general, system 4 has fully exploited many features of reactive ion techniques in semiconductor processing. The system can perform anisotropic plasma enhanced etching, deposition of good quality insulating films by MPECVD, and also can be combined with sputtering to deposit metal or metallic compound without heating the substrate.

2.6. System 5: The S.R. Mejia et.al System.

System 5 was developed in the Electrical Engineering Material and Devices Research Laboratory at the University of Manitoba, Canada. The system consists of a short circuited or matched stainless steel waveguide chamber. Two external coaxial coils are mounted around the waveguide chamber to provide a mirror like magnetic field along the axis of the waveguide. Figure 2.6 shows the overall system configuration. The magnetic field coils produce ECR conditions and are also used to confine the plasma in both the transverse and longitudinal directions of the chamber. The coils are water cooled. Microwave excitation is generated by a magnetron operating in a continuous mode at 2.45 GHz. The microwaves are guided by a WR-284 waveguide to a waveguide-coaxial adapter, a semirigid coaxial line, a coaxial waveguide adapter, and a directional coupler, and is finally fed into the waveguide chamber. The vacuum system uses a oil diffusion pump backed by a rotary pump. The base pressure is 10^{-6} torr. The primary pressure range of operation is between 10^{-1} to 10^{-4} torr. Under these conditions a low power plasma can be easily obtained. For example, maximum power absorption of 4 Watts and 32 Watts were used for a-Si:H films deposition and Si and SiO_2 etching respectively. The studies of etching and thin films deposited with the substrate surfaces parallel to the magnetic field lines can be found in references [10,11,12].

The system has undergone several improvements and is now being used to study dielectric thin film deposition. Currently the

substrate surface is normal to the axial magnetic field line. Thin films of a-Si:H and SiO_2 have been grown and characterized. Further information about films grown will be given in the following chapters.

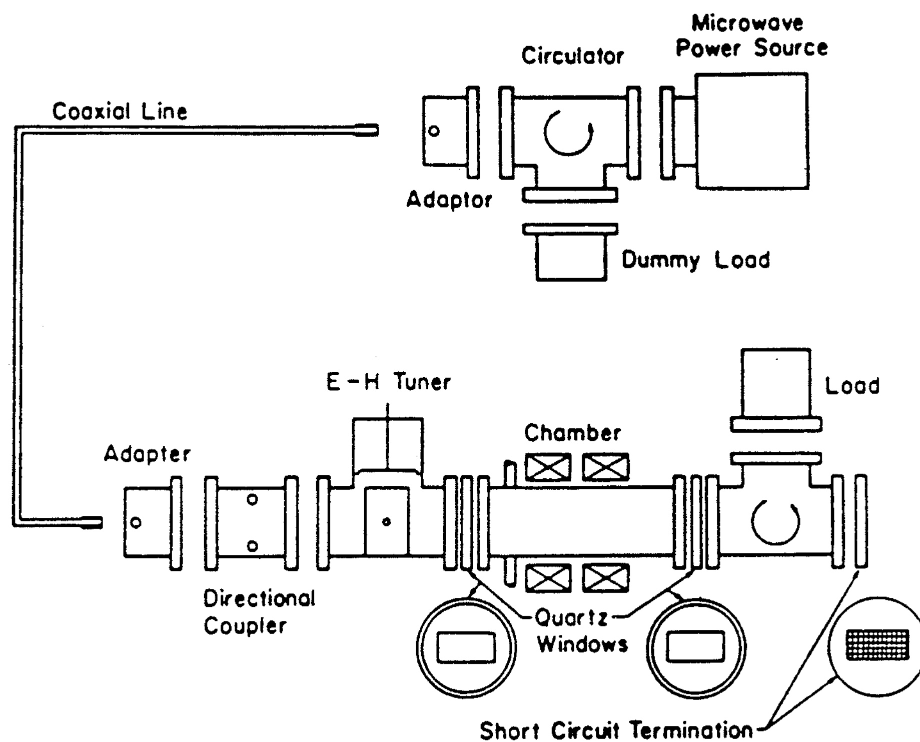

Figure 2.6: *ECR system developed at University of Manitoba.*

2.7. Conclusions.

In this chapter, various MECR systems have been briefly reviewed. Each system was discussed with respect to hardware design and areas of research. Some systems (eg. 1, 2, 3) are used for a specific purposes only (etching or deposition), but others, such as systems 4 and 5 are more flexible and applicable to several semiconductor processes such as MPECVD and MPECE.

2.8. References for Chapter 2

1 A. Chayahara, A. Masuda, T. Imura, and Y. Osaka. Jpn. J. Appl. Phys. 25(1986)l564.

2 T. Matsuda, H. Niu, M. Maeda, and M. Takai, Jpn. J. Appl. Phys. 25(1986)l425.

3 S. Matsuo and Y. Adachi, Jpn. J. Appl. Phys. 21(1982)l4.

4 K. Suzuki, S. Okudaira, N. Sakudo, and I. Kanomata, Jpn. J. Appl. Phys. 16(1977)1979.

5 S. Matsudo and M. Kiucji, Jpn. J. Appl. Phys. 22(1983)l210.

6 T. Ono, C. Takahashi, and S. Matsuo, Jpn. J. Appl. Phys. 23(1984)L534.

7 T. Ono, C Takahashi, M. Oda, and S.Matsuo, 1985 Symposium on VLSI Technology, pp-84-87.

8 S.R. Mejia, R.D. McLeod, K.C. Kao, and H.C. Card, Rev. Sci. Intrum. 57(1986)493.

9 N. Sakudo, K. Tokiguchi, H. Koike, and I. Kanomata, Rev. Sci. Intrum. 48(1977)762.

10 S.R. Mejia, T.T. Chau, R.D. Mc Leod, K.C. Kao, H.C. Card, to be published in The Canadian Journal of Physics.

11 S.R. Mejia, R.D. Mc Leod, W. Pries, P. Shufflebotham, D.J. Thomson, J. White, J. Schellenberg, K.C. Kao, and H.C. Card, J. Non-Cryst. Solids, 77&78(1985)765.

12 T.V. Herak, T.T. Chau, S.R. Mejia, P.K. Shufflebotham, J.J. Schellenberg, H.C. Card, K.C. Kao, and R.D. Mc Leod, J. Non-Cryst. Solids, 77&78(1987)227.

CHAPTER 3

MECR Plasma Etching

3.1 Introduction.

In the last few years, the rapid progress in VLSI devices has required that the minimum geometry features be reduced from the current 2 microns down to the submicron region. As such, the need for anisotropic etching techniques becomes increasingly important. Most researchers in the field have long believed that this need would be met by dry processing which relies upon a chemical reaction between some plasma species and the films resulting in a volatile product that can be pumped away. There are basically two types of dry etching processes, physical and chemical. Physical or sputtering techniques can cause damage and heating of the etched materials by impinging particles. Sputter-etched patterns are under sized, because the mask material is etched along with the substrate. On other hand, there is little damage or heating produced by chemical etching. In addition, by chosing appropriate discharge gases it should be possible to selectively etch only the desired material. Mixtures of CF_4 (carbon tetrafluouride) with O_2 (oxygen) have been widely used as plasma etchants. The discharge in CF_4 and O_2 plasmas produce fluorine atoms. The fluorine (F) atoms are believed to be the principal etchant for silicon etching. Flamm and et.al [1] conducted a silicon etching experiment using F_2 plasmas and showed that the silicon etch was linearly proportional to the F concentration. Other workers Coburn [2], Winters [3], and Mogab [4] also came to the same conclusion by studying mass spectroscopy and

OES of CF_4 and O_2 plasma discharges. In general they were able to correlate the fluorine atom concentration to the etch rate of silicon.

Radio frequency discharges of CF_4 and O_2 gas have been widely studied. However, microwave discharges of CF_4 and O_2 have not been as extensively studied. In this chapter we will discuss our studies of microwave plasma discharges of CF_4 and O_2 and compare these with rf plasma results. An OES system is used to monitor the fluorine atoms optical emission. The correlation of F atoms emission to etching rates is then obtained under various operating conditions. Parameters such as power, gas mixture, pressure, and magnetic field were adjustable in this study.

3.2 CF_4 Plasma and the Role of Oxygen in Fluorine Production.

In the absence of oxygen, it has been proposed that electrons in the discharge may decompose CF_4 principally via the following reactions:

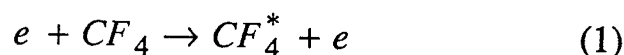

$$e + CF_4 \rightarrow CF_4^* + e \qquad (1)$$

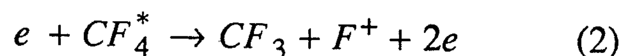

$$e + CF_4^* \rightarrow CF_3 + F^+ + 2e \qquad (2)$$

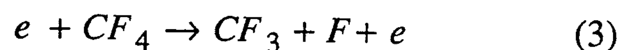

$$e + CF_4 \rightarrow CF_3 + F + e \qquad (3)$$

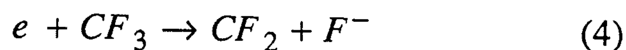

$$e + CF_3 \rightarrow CF_2 + F^- \qquad (4)$$

$$e + F^+ \rightarrow F \qquad (5)$$

In the discharge without oxygen, reaction (2) and (3) together with the detachment reaction (5) are apt to be the principle source of fluorine atoms. When no etching takes places, species are lost by recombination on the wall

$$CF_3 + F \xrightarrow{Wall} CF_4 \qquad (6)$$

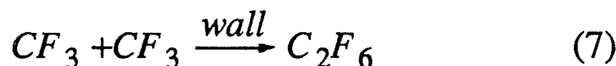

$$CF_3 + CF_3 \xrightarrow{wall} C_2F_6 \qquad (7)$$

$$F + F \xrightarrow{wall} F_2 \qquad (8)$$

or homogeneous recombination

$$CF_3 + F + M \rightarrow CF_4 + M \qquad (9)$$

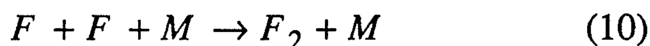

$$F + F + M \rightarrow F_2 + M \qquad (10)$$

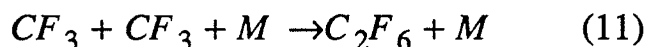

$$CF_3 + CF_3 + M \rightarrow C_2F_6 + M \qquad (11)$$

If silicon is present in a CF_4 discharge, Si atoms are removed by the etching process

$$Si + 4F \rightarrow SiF_4 \qquad (12)$$

Hence, F atoms that are removed by recombination, result in the suppression of the F concentration slowing down of the etch rate of Si. When oxygen is added to a CF_4 discharge, fluorine atomic concentration is increased significantly [1,2,3,4],

Typical OES spectra, as in Fig. 3.1a and Fig. 3.1b, show the CF_4 and $CF_4 + O_2$ discharge in our microwave ECR plasma. With about 10% added oxygen, one could increase the fluorine line (704 nm)intensity by about a factor of 10. This is in agreement with Coburn [2], Winters [3], and Flamm [1] who had studied and recorded F concentration via OES and mass spectroscopy during plasma etching of silicon.

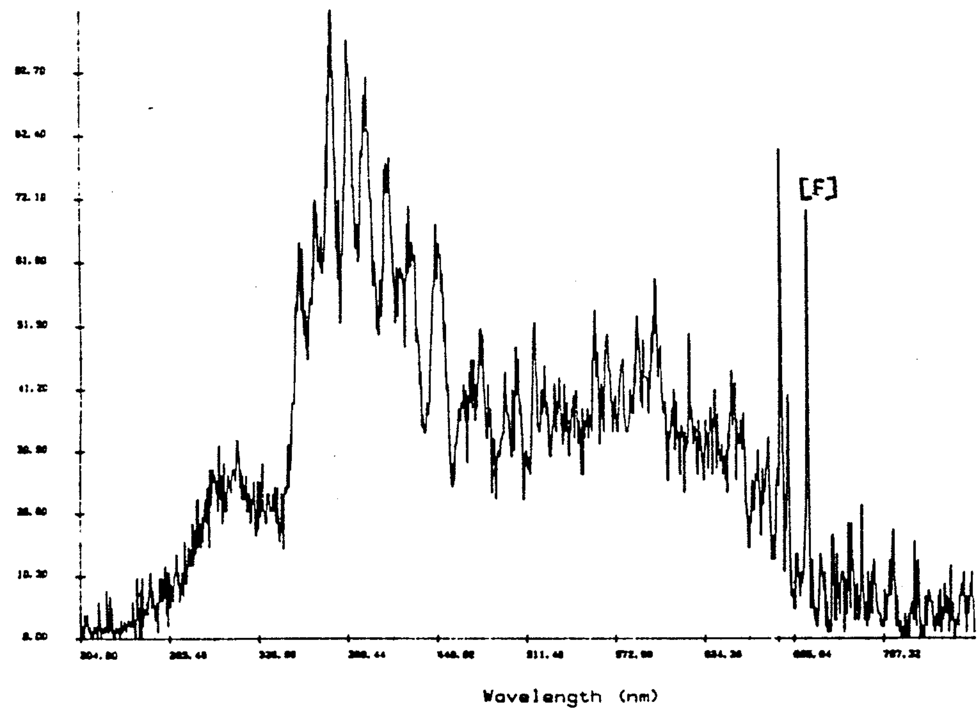

Figure 3.1a *OES Spectrum of CF_4 plasma in the absence of O_2.*

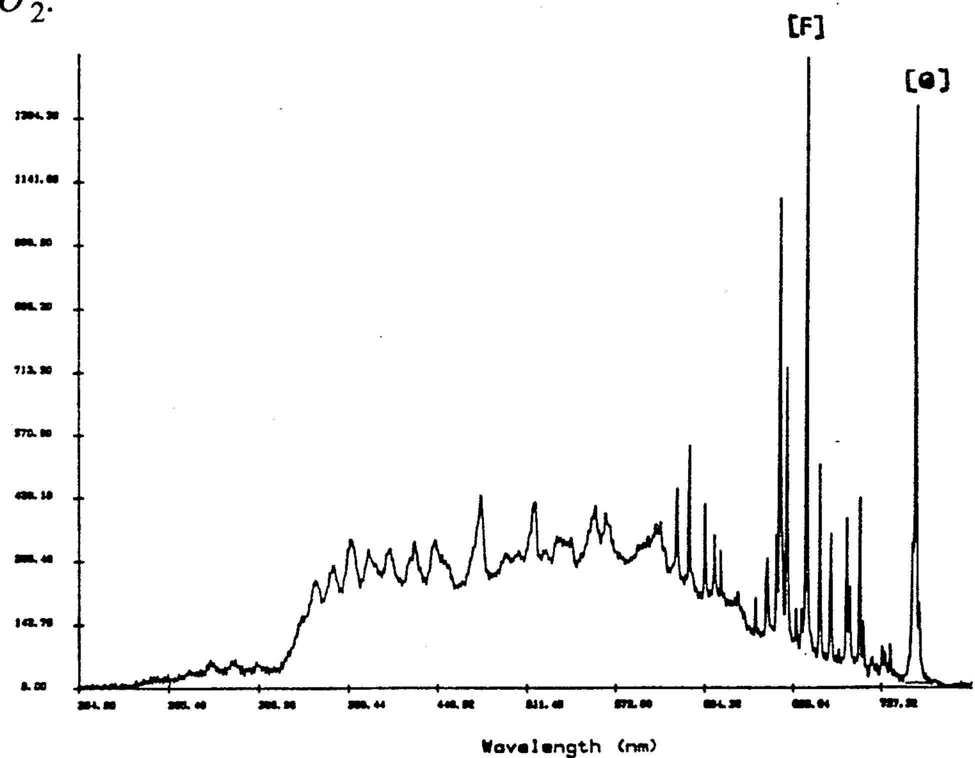

Figure 3.1b *OES Spectrum of CF_4 plasma with 10% of Oxygen added.*

The role of oxygen in fluorocarbon glow discharges is to react with carbon to form CO, CO_2, or COF_2 [1,3]. This has the effect of increasing the effective F atom concentration. There are several plausible explanations proposed for the increase in F concentration due to the added oxygen [3,4].

1 Oxygen retards the heterogeneous recombination of F atoms with other species either by reacting with them or by blocking access to a favorable recombination surface.

2 Oxygen retards the rate of the homogeneous reaction of F atoms with other species by depleting the reactants via oxidation.

3 Oxygen retards the loss rate of fluorine such as F^- by removing species which would otherwise consume the precursors.

4 Oxygen reacts with fluorine-containing species to liberate F atoms. The reaction may occur on the surface or in the gas phase.

3.3 Properties of Dry Etching.

In general, plasma etching processes can be classified according to etch rate, selectivity, anisotropy, and the degree of the loading effect. Practical etch rates (in rf systems) are between 100 Å/min to 10,000 Å/min. Selectivity refers to the ratio of the etch rates between two different materials to be etched in the same plasma, for example Si and SiO_2 which may be simultaneously present on a single wafer. Anisotropic etching refers to etching that can be rapid in a direction normal to the surface of a wafer, but slow in a direction parallel to the wafer surface. Thus it is possible to etch a small pattern with steep vertical walls. The loading effect refers to a substantial depletion of the reactive plasma etching species brought about by rapid consumption of this reactant in the etching process. As the amount of material being etched is increased, the rate of etchant removal from the gas phases increases and the steady state reactant concentration decreases, thereby lowing the etch rate. In our experiment, we have reduced the loading effect by placing several dummy substrates inside the chamber during etching, thereby keeping the loading effect constant from run to run.

3.4 Experimental.

In this work, we studied the etching of Si and SiO_2. The etchant was a mixture of CF_4 and O_2 gases. The system configuration was described in Chapter 2 (system 5). The gas mixture of CF_4 (99.7% pure) and O_2 (99.98% pure) was introduced into the discharge chamber after evacuation to 5×10^{-6} torr. Silicon wafers (N-type, 0.5 - 1 ohm - cm, (111) surface) and SiO_2 (quartz transparent substrates, Quartz Scientific Inc, nominal purity of 99.98%) were etched in positions parallel to the magnetic field lines. The masks consisted of vacuum deposited aluminum (600 Å) patterned by conventional photolithography on the substrates. The etch rate was calculated from the change in the step height at the edges of the mask. The steps were measured using a Sloan Dektak surface Profilometer. The directionality and surface aspect were determined by Scanning Electron Microscope (SEM). Axial optical emission from the plasma was sampled through a quartz window. A set of quartz lenses and mirrors focussed the light on a 25 μm slit of a 30 cm Jarrel-Ash Spectrometer, which was equipped with a 1200 groove/nm grating and a 1024 diode array and a EGG-PARC multi-channel analyzer. Microwave power absorption (P_A) was measured by an Hewlett Packard dual power meter. Pressure was measured using a capacitance manometer.

3.4.1. Etching Rate versus Fluorine Concentration.

In this experiment, we compared our findings to other workers' regarding the nature of atomic fluorine in etching of Si and SiO_2. The OES spectrum of CF_4 and O_2 plasmas were studied by monitoring the atomic fluorine and oxygen lines, [F] at 704

nm and [O] at 772 nm respectively. As a result, very high etch rates 0.76 μm/min for Si and 0.17 μm/min for SiO_2 were achieved by maximizing the neutral fluorine emission peak. The operating parameters were total pressure (P_T) of 0.8 torr, oxygen partial pressure P_o of 14%, absorbed microwave power P_A of 32 Watts, and a normalized magnetic field of 1.48. The result suggests that in a CF_4 and O_2 microwave ECR plasma system, the fluorine atoms are a major etchant for Si and SiO_2 as similarly found in rf plasma systems.

3.4.2. Etch Rate as a Function of Oxygen Concentration.

In this section we will continue the discussion of the role of oxygen in etching Si in a CF_4 plasma. The addition of small amounts of O_2 increase the F concentration and as a consequence the etching rate of silicon. However, the over abundance of oxygen can also depress the Si etch rate. Figure 3.2 shows the etch rate of Si and SiO_2, the emission intensity from excited fluorine atoms, [F], and oxygen atoms, [O], as a function of the percentage of O_2 partial pressure at P_T of 0.8 torr, NMF (normalized magnetic field) of 1.09 and P_A of 10 Watts. From Fig. 3.2 the etch rate of Si and the [F]/[O] ratio drop dramatically with the increasing oxygen partial pressure beyond 10%. Both curves follow similar trends, while the etch rate of SiO_2 remains unchanged. A simple model of the etching has been proposed [3, 4] to explain this phenomena, that is: with the excessive O_2 in the plasma, the freshly exposed silicon surfaces are oxidized by atomic oxygen. The chemisorption of oxygen atoms on the Si surface would slow down the etch rate of Si. This phenomena is also observed in rf plasma etching systems where the silicon etch rate

also decreases with the decreasing [F]/[O] ratio.

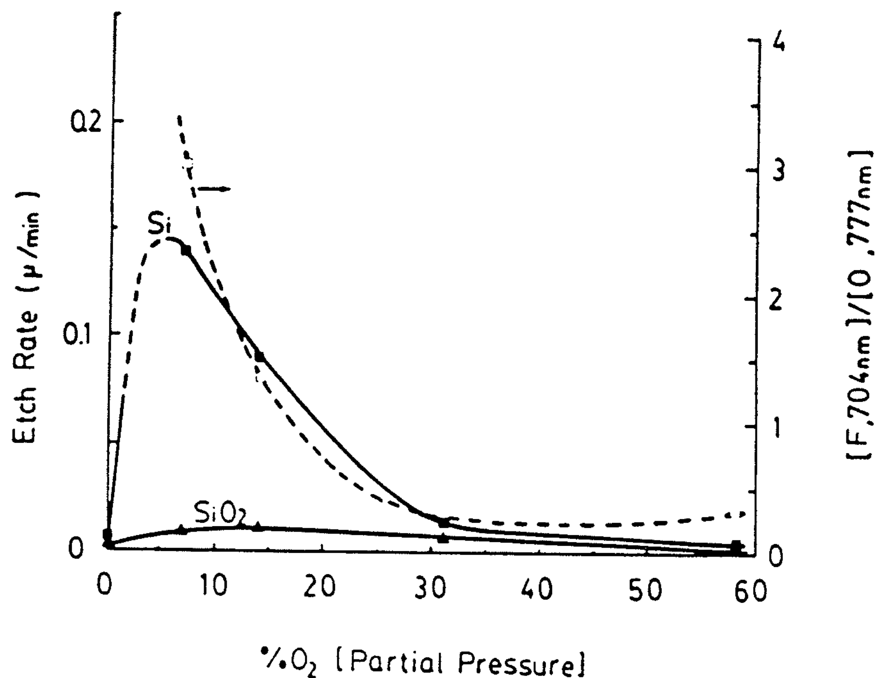

Figure 3.2 *Etch rate and [F]/[O] ratio as a function of O_2 concentration.*

Hence, as in an rf system, oxygen is seen to have a dual role in etching of Si. It enhances the production of the etchant [F] in the plasma, and it retards the etching reaction by adsorbing on active surface sites. These two processes have opposing effects on the etch rate and the net result is that the etch rate reach maximum value at a relative low concentration of O_2 in the feed gas.

3.4.3. Power Dependence.

The dependence of etch rate on power absorbed, at P_T of 0.8 torr, P_O of 14%, and NMF of 1.09, is shown in Fig 3.3. The etch rate of Si follows closely the [F]/[O] ratio, suggesting that

more neutral atomic fluorine is produced with increasing power. However, under very high power absorption, more energetic particles will be present inside the plasma. As the results indicate, the surface of the substrate now is heavily bombardment by energetic particles. Although the bombardment will assist the acceleration of the etching mechanisms, it also induces damage to the substrate surface. Figure 3.3 shows the rough surface of Si wafer after being etched at 32 Watts of absorbed power where the maximum etch rate was 0.74 μm/min.

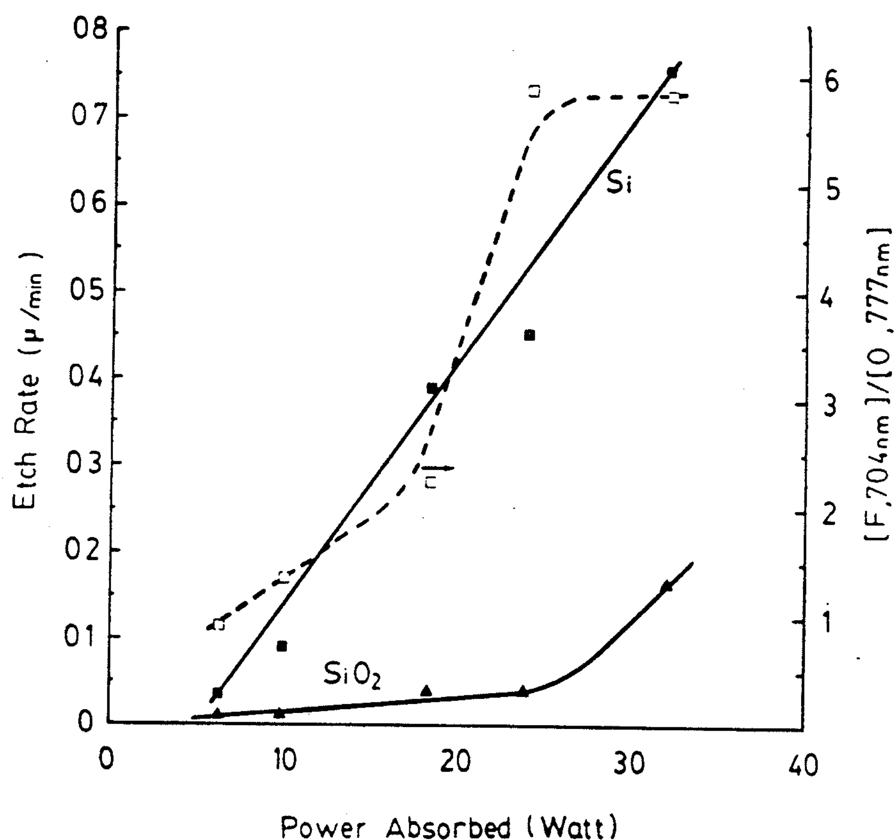

Figure 3.3 *Etch rate as a function of Power.*

Figure 3.4 *Very rough surface of Si after etch under high Power Absorption.*

3.4.4. Pressure Dependence.

Si and SiO_2 etch rates as function of total pressure (P_A of 10 Watts), NMF of 1.09, P_O of 14% are shown in Fig. 3.6. The Si etch rate falls by approximately 30 times when the pressure is reduced from 10^{-1} to 10^{-2} torr. The 3 nm/min Si etch rate at 10^{-3}

torr is much lower than the 46 nm/min etch rate reported by K. Suzuki and et.al [7] in an ECR microwave ion source system without ion screening. It is however comparable to the 1 nm/min that they reported with ion suppression. These results imply that the magnetic field effectively confines the ions, playing a role similar to the ion screening or suppression in [7]. With the ion screening effect of the magnetic field, etching of Si is due mainly to neutral active species, which are appreciably reduced at 10^{-3} torr. The 100 nm/min etch rate at 10^{-1} torr is an order of magnitude larger than the etch rate reported in [7], possibly due to a closer plasma to substrate distance in our experiment. This is, in spite of having an order of magnitude lower microwave power in our work.

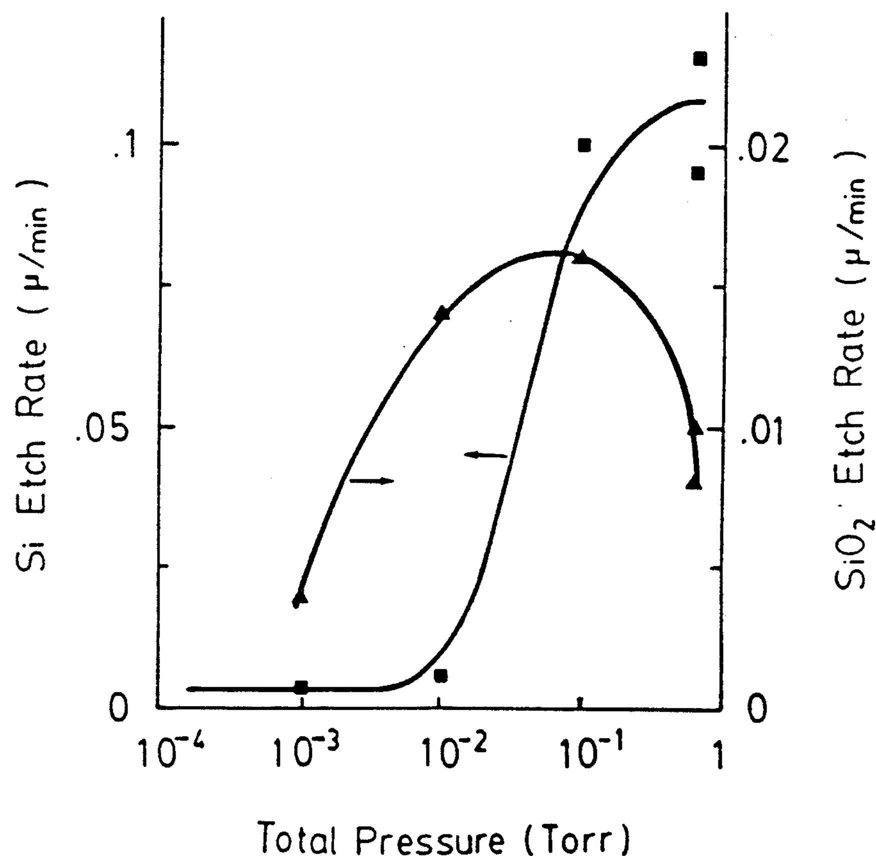

Figure 3.6 *Etch rate as a function of Pressure.*

The SiO_2 etch rate is about 15 nm/min at 10^{-1} torr but drops to 3 nm/min at 10^{-3} torr. These values can be compared to with 36 nm/min and 1 nm/min respectively for the case without ion screening [7], as SiO_2 etching is believed to be carried out mainly by neutral species. These trends can be explained in term of the reduced ion impingement at low pressure, and the smaller substrate to plasma distance in our work.

3.4.5. Magnetic Field Dependence.

The magnetic field dependence of Si and SiO_2 etch rates at P_T of 0.8 torr, P_O of 14% and P_A of 10 Watts are shown as Fig 3.7. The undercutting parameter a/b for Si, as defined in the same figure, and the [F]/[O] ratio is also plotted as a function of NMF. A 50% increase in the etching rate is observed at a NMF = 1.32. The undercutting and the [F]/[O] ratio as a function of NMF seem to follow similar trends. The unusual enhanced undercutting that was observed may be caused by carbon coverage of the unmasked surface [6]. A increase of the [F]/[O] ratio implies a larger supply of carbon-containing species and an insufficient supply of atomic oxygen to prevent the carbon deposition. As a consequence the vertical etching rate is slightly reduced as shown in the bottom part of Fig 3.7. The lateral etch rate increases with the increased atomic fluorine concentration, being unimpeded by a greatly reduced amount of carbon under the mask. The reduced carbon under the mask could be explained if the main source of carbon were low energy ionic radicals, since these ions would be accelerated without collision across the plasma sheath in a path normal to the surface. While there is experimental evidence of the contribution of the CF_3^+ low energy

ion to the carbon film deposition [3], neutral species containing carbon may also play an important role . This carbon coverage explanation is consistent with the observed isotropic nature of the SiO_2 etching at all pressure, and with the isotropic Si etching profiles observes at low pressure.

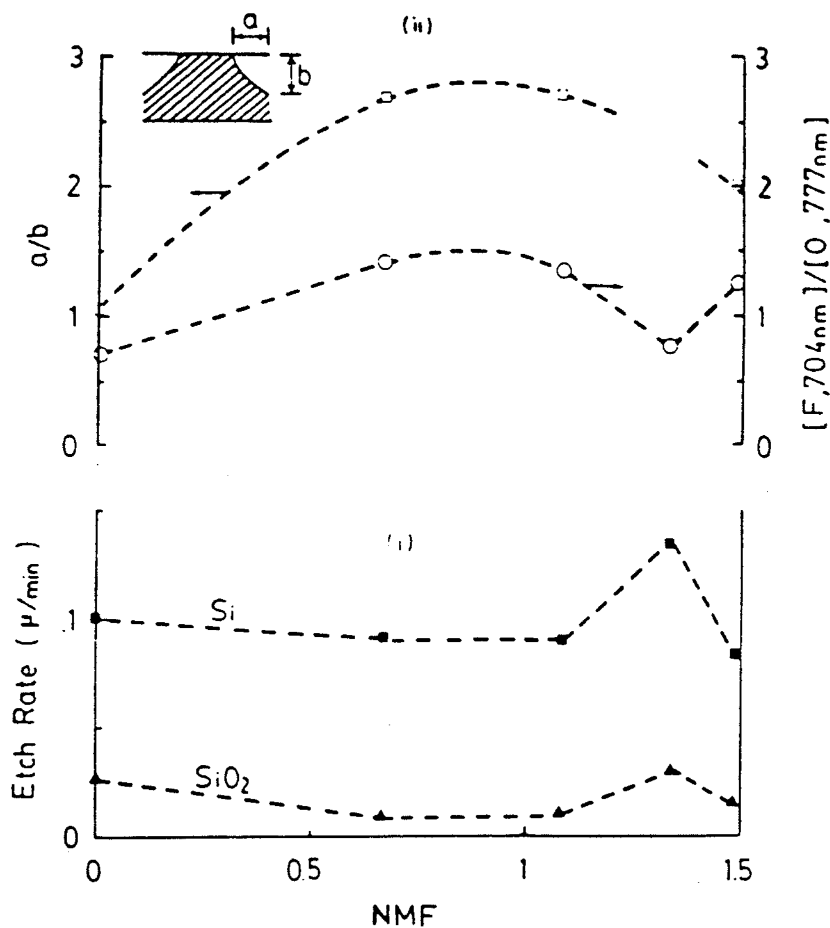

Figure 3.7 *Etch rate as a function of Magnetic field and [F]/[O].*

3.5 Conclusions.

Si and SiO_2 etching in a CF_4 and O_2 ECR microwave plasma exhibit mechanisms similar to those found in rf systems and ECR microwave ion sources used with ion suppression. In the present system, we employed a DC axial magnetic field for plasma confinement, with the magnetic field vector parallel to the substrate surface. The main active species for Si etching seem to be neutral atomic fluorine. Very high etching rate are achieved at high pressure (0.8 torr) and high power (32 Watts). The etching of Si is isotropic at high pressure in the absence of DC magnetic field, but the undercutting increases with the applied magnetic field. This implies an increased carbon coverage on the horizontal surface which in turn reduces the vertical etching, while the lateral etching is enhanced by the profuse supply of atomic fluorine acting on the relatively carbon free vertical surface.

3.6 References for Chapter 3.

1 D. L. Flamm, Solid State Tech. April 1979, pp-111-116.

2 D. L. Flamm, Vincent M. Donnelly, and John A. Mucha, J. Appl. Phys. 52(5), May 1981, pp-3633-3639.

3 J. W. Coburn, H. F Winters, and T. J. Chuang, J. Appl. Phys. 48(8), August 1977, pp-3532-3540.

4 C. J. Mogab, A. C. Adams, and D. L. Flamm, J. Appl. Phys. 49(7), July 1978, pp-3769-3803.

5 J. W. Coburn, Eric Kay, Solid State Technol. April 1979, pp-117-124.

6 S. R. Mejia, T. T. Chau, R. D. McLeod, K. C. Kao, and H. C. Card, to be published in the Canadian Journal of Physics.

7 K. Suzuki, S. Okudaira, and I. Kanomata, J. Electrchem. 126(6), 1979, pp-1024-1028.

CHAPTER 4

a-Si:H Thin Film Deposition.

4.1 Introduction.

Hydrogenated amorphous silicon (a-Si:H) thin films have been studied for many years. The conventional deposition method of prepairing a-Si:H films is rf plasma excited CVD. Although film deposition by rf plasma techniques results in desirable optical and electronic properties, the deposition rates associated with high quality films have remained low. Microwave plasma systems with magnetic field confinement have been demonstrated to be alternatives for the deposition of a-Si:H. In particular, ECR microwave plasmas feature high deposition rates and good quality films due to a more complete gas dissociation [1,2]. Power requirements and the operating pressure range have also been reduced.

A previous method of thin film deposition studied here was with the substrate surface held parallel to the magnetic field lines [2]. Consequently, ion bombardment was not expected to play an important role in governing the properties of deposited films, because of magnetic screening effects [3]. However, in rf PECVD studies it has been shown that ion and electron bombardment do in fact play a desirable role in the fabrication of high quality deposited films [4,5]. This bombardment is also expected to play an important role in MECR plasmas. In the present study, we report the experimental results of the effect of substrate bias during films deposition upon the structural, optical, and electronic properties of thin film a-Si:H.

4.2 Experimental.

a-Si:H films were deposited using the ECR microwave system described in chapter 2 (system 5) with the following modification. A thermostatically controlled stage or table was positioned above the diffusion pump port, Fig. 3.1, allowing the substrate surfaces to be held normal to the DC magnetic field in the region of diverging magnetic field lines remote from the plasma. The table was maintained at a constant potential ranging from -300 V to 100 V during deposition. The plasma was maintained at a fixed distance ($\approx$ 10 cm) from the stage by the magnetic field peak position of a single coil. The microwave power was fed into the chamber in the TE_{10} mode at the opposite end of the chamber. A quadrapole mass spectrometer and an optical emission spectrometer were used to monitor the gas composition and its dissociation. Langmuir probes were used to monitor the variation of the plasma properties as a function of the deposition conditions. Gas flow was controlled with mass flow controllers and chamber pressure was monitored with a capacitance manometer. Film growth was monitored in situ by laser interferometry.

Films were deposited from a 10% SiH_4 and 90% H_2 mixture, total flow rate 22 sccm, substrate temperature 250°C, total pressure of 10^{-3} torr, and microwave absorbed power of 4 Watts. The chamber was baked at 200°C and evacuated by a diffusion pump with a cold trap held at liquid nitrogen temperature before deposition. The ultimate vacuum was better than 10^{-6} torr. During deposition the chamber temperature was lowered to 160°C. Films were also deposited on the chamber walls, directly below the plasma with their surfaces parallel to the magnetic field.

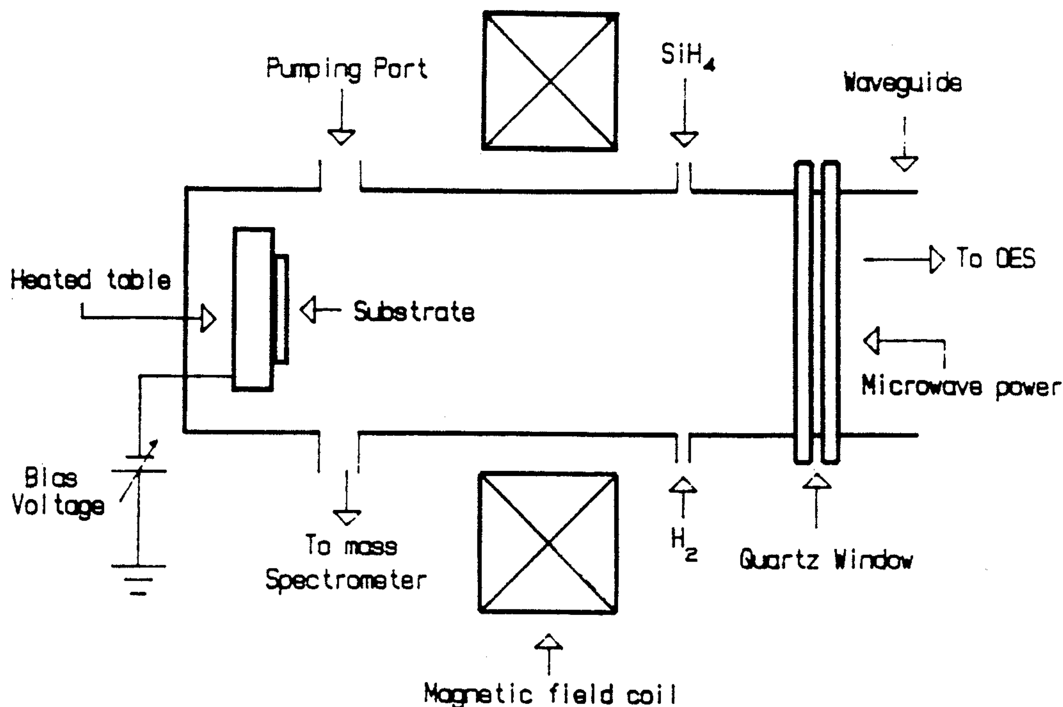

Figure 4.1 *Modification Chamber for a-Si:H films growth study.*

Films were characterized by spectrally resolved ellipsometry, dark conductivity and photoconductivity measurement, X-ray diffraction, FTIR, and scanning electron microscopy. Quartz, stainless steel, and c-Si substrates were employed for comparisons under otherwise identical deposition conditions. Films thickness ranged from 1 to 3 μm.

4.2.1 Substrate Potential, Deposition Rate versus Table Bias.

The average energy of incident ions on a substrate is generally determined by the difference between the plasma potential V_p, and the potential of the substrate which may be at an applied potential or bias V_b, or at the floating potential V_f, in the discharge. In this study, quartz substrates maintain the potential V_f, while the stainless steel substrates maintain the bias potential V_b. It is assumed that the surface of the growing film is at the potential of the substrate surface. Figure 4.2 illustrates the variation in the incident ion energy, E_{ion}, as the stage or table bias is varied from -300 V to 100 V DC in an H_2 plasma. Similar trends have been observed in a SiH_4 and H_2 plasma but with absolute values some what reduced ($\approx$ 10%). For the quartz substrates, there is little variation in E_{ion}, which depends upon V_p - V_f, as the table bias is varied. For the stainless steel substrates E_{ion} varies as V_p - V_b, and is seen to increase with negative table bias.

The deposition rate, r_d, for films deposited on quartz and stainless steel substrates as a function of table bias are shown in Fig. 4.3. The deposition rate for the films deposited on quartz is approximately 2.3 Å/sec independent of table bias. For the stainless steel substrates, the film growth rate at 0 V table bias is comparable to that for the quartz substrates and then increases as the negative bias increases to moderate values, and finally decreases for high negative bias voltages. The r_d for films grown on quartz are consistent with the almost constant ion energies expected for a floating surface. For films grown on stainless steel substrates, the increases in r_d at low ion energy may be explained by an increased surface reaction rate if this reaction is energy activated.

Further increases of ion energy would reduce the deposition rate due to etching of the growing film surface.

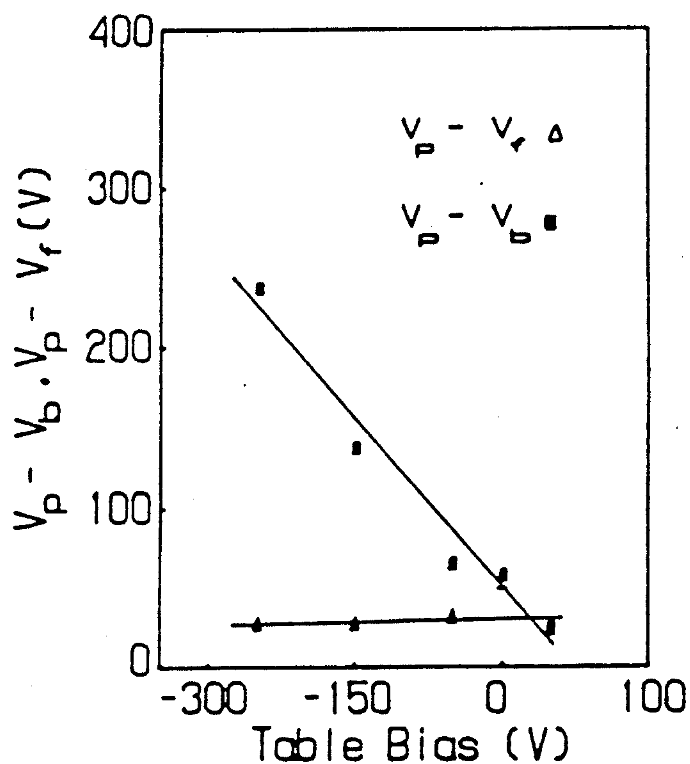

Figure 4.2 *Difference between the plasma potential and the floating potential* V_p - V_f, *and between the plasma potential and the table bias voltage* V_p - V_b, *as functions of* V_b.

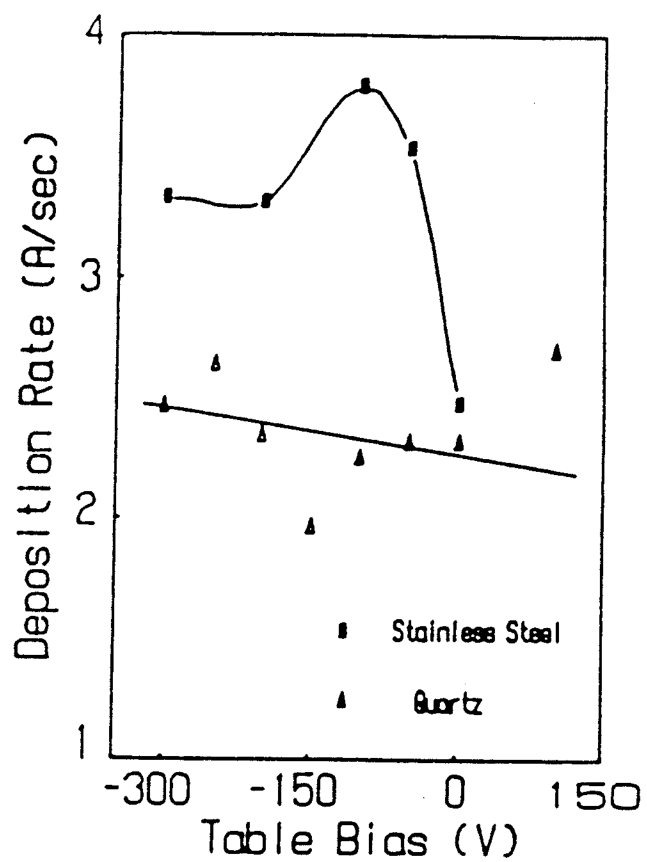

Figure 4.3 *Deposition rate as functions of bias voltage.*

4.2.2 ε_2 and the Conductivity veresus Table Bias.

Figure 4.4 illustrates the maximum in the imaginary part of the dielectric constant ε_2 obtained from ellipsometric measurements.

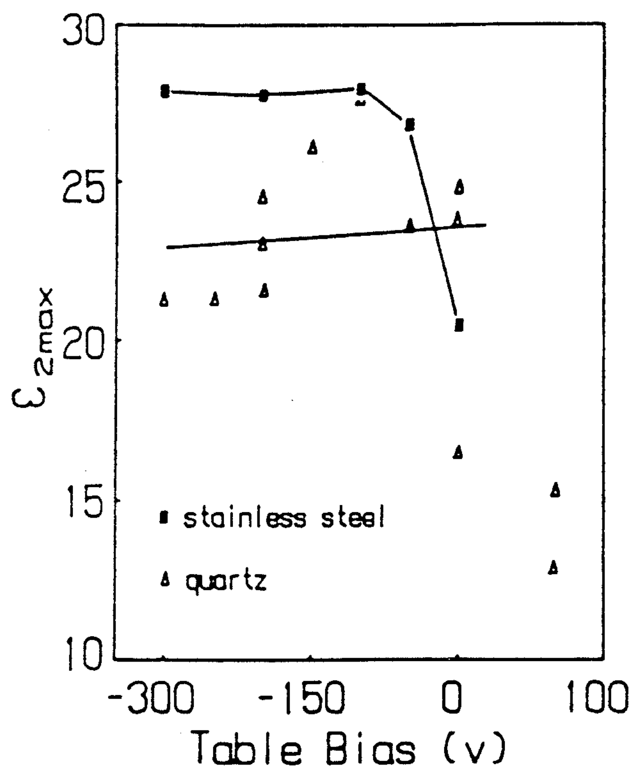

Figure 4.4 ε_{2max} *against table bias.*

The relative high values of ε_{2max} are indicative of high density a-Si:H as reported elsewhere [6], in addition the position of the peak in the ε_2 spectra does not appear to be significantly effected by the table bias indicating little or no surface roughness attributable to the ion bombardment [7]. Under negative table bias, the films deposited on the stainless steel substrates consistently demonstrated a larger value of ε_{2max} as opposed to their quartz substrate counterparts. These results are consistent with the incident ion energy data of figure 4.2, where the ion

bombardment during film growth has resulted in film densification. For positive table bias, substantial numbers of electrons are withdrawn from the plasma region which may give rise to an increased ion bombardment of the surrounding structure as well as reduced ion bombardment of the growing film itself resulting in generally low density and poor quality film [8].

Figure 4.5 illustrates the ratio of photoconductivity to dark conductivity, σ_{ph}/σ_d, and σ_d as a functions of the table bias for both stainless steel and quartz substrates.

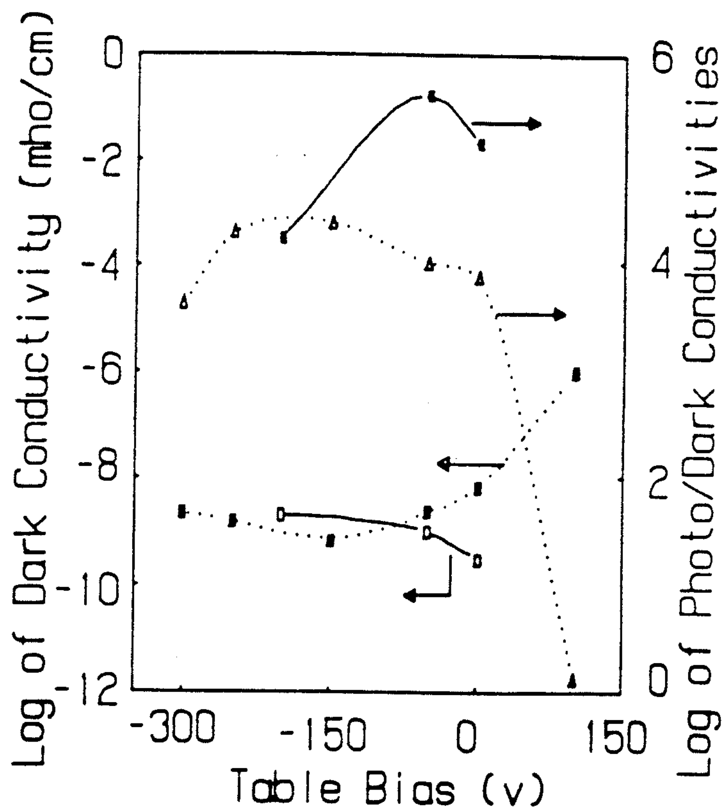

Figure 4.5 *Dark conductivity and σ_{ph}/σ_d as a function of table bias.*

For films deposited under negative table bias typical value of σ_d are seen to be on the order of 10^{-9} $(\Omega\ cm)^{-1}$ comparable to high quality of rf deposited films. As anticipated, films deposited

under positive table bias with poor optical properties also displayed poor electrical properties. The photoconductivity was measured at a wavelength of 6328 $\mathring{A}$ with a photon flux of 10^{15} photons-s^{-1}-cm^{-2}. In a similar manner the films with good optical properties also displayed photoconductivity typical of good quality films.

FTIR of the films deposited with negative bias show a single peak at 2000 cm^{-1} corresponding to the SiH stretching mode. Peaks at 2100 cm^{-1} have not been detected suggesting the absence of SiH_2 bonds. Hydrogen content has been estimated to be 6 to 7%. No features due to oxygen or other contaminants were observed. Films deposited on substrates at the walls of the chamber, just below the plasma, with their surfaces parallel to the magnetic field consistently showed low density, poor photoconductive properties, and hydrogen incorporation in both SiH_2 and SiH bond configurations. Hence the lack of ion bombardment due to ion screening results in poor properties.

4.3 Conclusions.

In general, films deposited with their substrate surfaces normal to the magnetic field lines exhibited good optical and electronic properties, even in the absence of an applied bias. This can be explained by moderate ion bombardment due to the escape of ions toward the substrate table along the fringing magnetic field lines. A moderate bias increased the deposition rate, the film density, and the optical and electronic quality of the films. Moderate ion bombardment of the growing film is seen to be a necessary condition for good quality a-Si:H film deposition.

4.4 References for Chapter 4

1 S.R. Mejia, R.D. McLeod, K.C. Kao, H.C. Card, J. Non-Cryst. Solids, 59 & 60, (1983), 727-730.

2 S.R. Mejia, R.D. McLeod, W.Pries, P. Shufflebotham, D.J. Thomson, J. White, J. Schellenberg, K.C. Kao, and H.C. Card, J. Non-Cryst. Solids, 77 & 78, (1985), 765-768.

3 S.R. Mejia, T.T. Chau, R.D. McLeod, K.C. Kao, and H.C. Card, to be published in The Journal of Canadian Physics.

4 B. Drevillon, J. Huc, and N. Boussarssar, J. Non.-Cryst. Solids, 59 & 60, (1983), 735-738.

5 F.A. Saroff, Z. Iqbal, and S. Veprek, Solid State Com., 42(6), pp. 465-468, 1982.

6 B. Drevillon, J. Huc, A. Lloret, J. Perrin, G. de Rosny, and J. P. M. Schmitt, Appl. Phys. Lett., 42, (1983), 801.

7 B. Drevillon and F. Vaillant, Thin Solid Films, 124, (1985), 217.

8 J.W. Coburn and E. Kay, J. Appl. Phys., 43, (1972), 4965.

CHAPTER 5

Silicon Oxide Deposition

5.1 Introduction.

In addition to etching and deposition of hydrogenated amorphous silicon, there is increasing interest in low temperature processing of SiO_2 films grown by plasma enhanced CVD. Along these lines SiO_2 films have been grown at 200–500^oC in rf plasmas systems from SiH_4 and N_2O gas mixtures [1, 2]. In some cases the physical and electrical properties were close to those of thermal oxide grown at 1000^oC [3, 4]. However, the films produced using SiH_4 and N_2O plasmas normally contain SiH, SiOH, NH, and SiN groups [5]. Another PECVD method of growing SiO_2 film is using SiH_4 and N_2O in a down stream configuration [11]. In this case, an oxygen plasma is produced in a separate chamber and transported down to a deposition chamber were it reacts with SiH_4 to form SiO_2 film. Some workers [7,11] reported that films grown in the down stream mode are near stoichiometric SiO_2 with less than 1 at % H. However, most of the systems use pressures on the order of 0.1 torr and the SiH_4 is diluted by He or Ar gas to avoid a spontaneous violent reaction between SiH_4 and O_2.

In this chapter, we present the preliminary study of SiO_2 film deposition in an ECR Microwave plasma system [6] using SiH_4 and O_2 gases. The films are deposited at a pressure of 10^{-3} torr without SiH_4 being diluted. No film or powder formation has been observed when SiH_4 and O_2 are fed to chamber at this pressure without microwave excitation. Films have been deposited on

substrate with their surface parallel to the magnetic field lines at 200 ± 5° C. The FTIR absorption spectrum have not shown absorptions due to SiH or SiOH groups. The IR absorption bands look similar to those of thermal oxide grown at 1000° C with absorptions at 1060 cm^{-1},800 cm^{-1}, and 450 cm^{-1} for Si-O-Si stretching, bending, and rocking vibration respectively.

Film deposition and etch rates were studied as functions of substrate positions relative to the plasma volume. The results were then compared to the properties of films grown on substrate with their surfaces normal to the axial magnetic fields from the same plasma [4].

Annealing of the films at 1000° C for 30 min under N_2 atmosphere was also studied to observe the change of film properties. The IR spectrums of the annealed films were comparable to those of thermal grown films at 1000^0C in dry O_2 with the main stretching frequency occurring at 1080 cm^{-1}.

5.2 Experimental.

SiO_2 films were deposited on p-type, 60 ohm-cm, (100) c-Si wafer. System modifications and substrate positions are shown in Fig 5.1. The substrate position was defined as zero when the substrate is inside the middle of magnetic field coil position as shown. The chamber was heated and held at 200±5° C before and during deposition. The base pressure was 10^{-6} torr. In an attempt to avoid (or reduce) direct dissociation of SiH_4 inside the chamber, an oxygen plasma was generated at the power input end and SiH_4 was injected at the pumping port end.

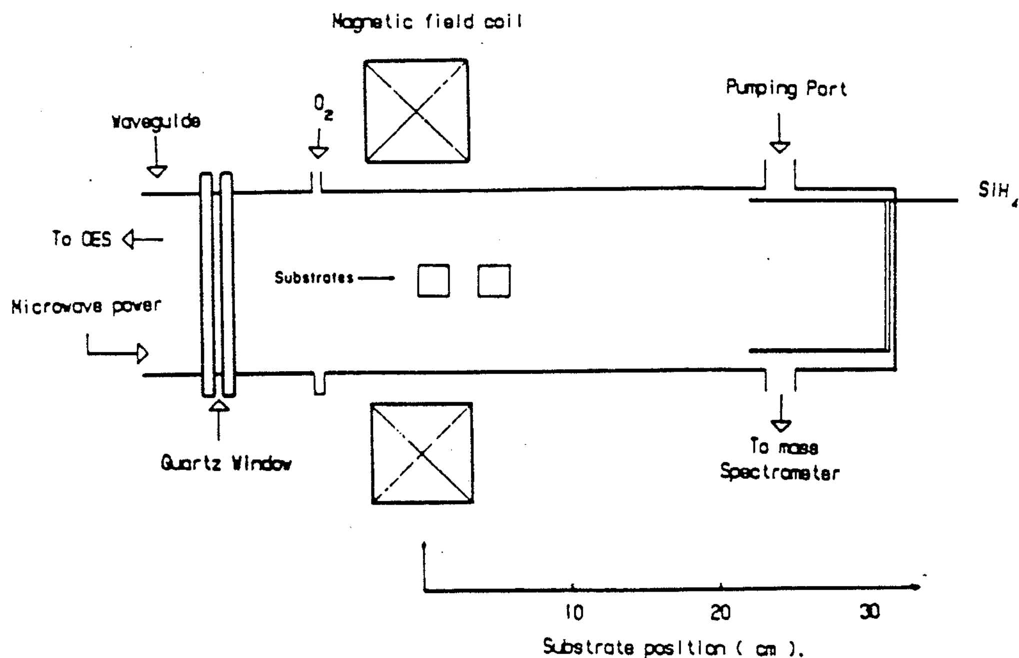

Figure 5.1 *Chamber modification for SiO_2 film growth.*

With this configuration, we anticipated that films grown inside the chamber would be due to a plasma reaction of oxygen and SiH_4 species at one end (under the magnetic field coil), gas phase reaction of SiH_4 with active radicals of oxygen at other end (near pumping port), and a combination of both at the middle perhaps.

Films were deposited at 10^{-3} torr and gas flow of 1 sccm and 10 sccm for SiH_4 and O_2 respectively. The external magnetic field current was 22 Amps which provided the ECR condition of 875 G. Power absorption was 8 Watts. Films were characterized by a Bomen Michelson FTIR 100 Spectrophotometer with resolution of 5 cm^{-1}. Wet etching was done in a P-etch solution of HF:15, HNO_3:10, H_2O:60. Film thickness ranged between 900 Å - 1500 Å, measured by Sloan Dektak surface profilometer. Refractive index and thickness values were also obtained by ellipsometry at wavelength of 6328 Å.

5.2.1 Deposition Rate versus Substrate Position.

Figure 5.2 shows the deposition rate versus substrate position. The deposition rate is constant inside region between 0 to 11 cm and drops after the 11 cm point. There is a sharp reduction of deposition rate at distance where the substrate is about λ_0 (λ_0 is mean free path about 8 - 10 cm at 1 mtorr) away from the plasma volume. Consequently, the high deposition rate in region 0 - 6 cm is thought due mainly to reaction of both active radical of oxygen and silane produced in the microwave plasma. As the substrate is moved further away from the plasma discharge, the dominant active species are reduced until a point where the reaction now is thought to be due to gas reactions of silane with

reactive radicals of oxygen alone. The reduced deposition rate in the region 14-16 cm is though to ocur in the same manner to that of downstream reactions.

These results are in agreement with the results from films grown in positions normal to axial of the magnetic field line as reported by Herak[4]. In [4] the deposition rate was studied as a function of the coil position. They had detected the reduction of deposition rate when the coil was far away from the substrate.

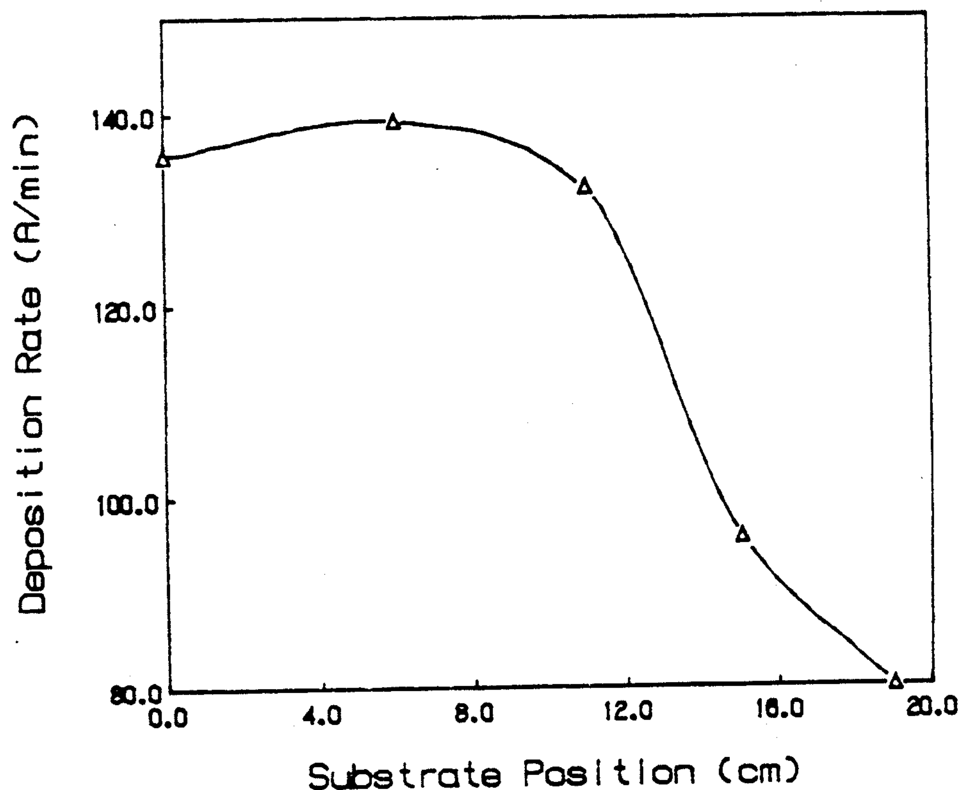

Figure 5.2 *Deposition rate versus substrate position.*

5.2.2 FTIR Absorption Spectrum.

In Fig 5.3, the room temperature infrared absorption spectrum of an as-deposited SiO_2 film, is shown. Intense absorption is noted in region 400 cm^{-1} to 1400 cm^{-1}. The Si-O-Si stretching, bending, and rocking modes are observed at 1060 cm^{-1}, 800 cm^{-1}, and 450 cm^{-1} respectively. These results are similar to other work reported on SiO_2 PECVD film deposition [7], [8]. No other intrinsic absorption was found in the region between 1400 - 4000 cm^{-1} indicating no SiH, SiOH or OH groups.

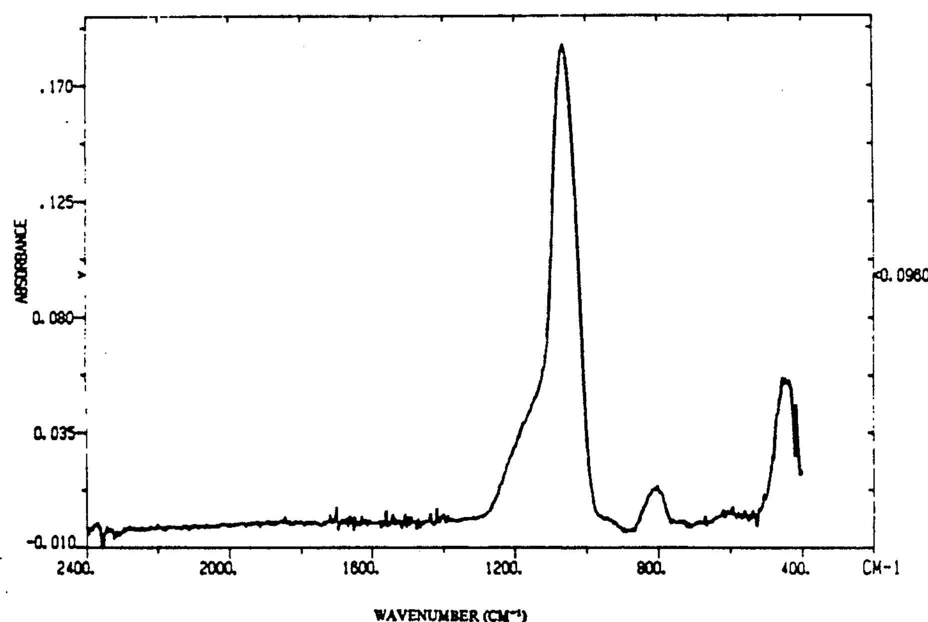

Figure 5.3 *IR absorption spectrum of an as-deposited film.*

For all of the as-deposited films at different positions, the peak positions γ_m of the Si-O stretching mode was found between 1060±5cm^{-1}. The half maximum width Δ_m was between

$80 \pm 5 cm^{-1}$. Figure 5.4 shows that there is no correlation between the film position to γ_m or Δ_m. This result also agrees well with work reported by Herak [4].

The absorption defined as $\log_{10}(I_0/I)$, where I_0 and I are the incident and transmitted intensities respectively was determined at each maximum absorption using the base line method and is plotted as a function of film thickness in Fig 5.5. A linear relationship is obtained for the observed band 1060 cm^{-1}, and indicates that the Lambert Bouger's law is obeyed in the range of thickness studied (900 - 2000 Å).

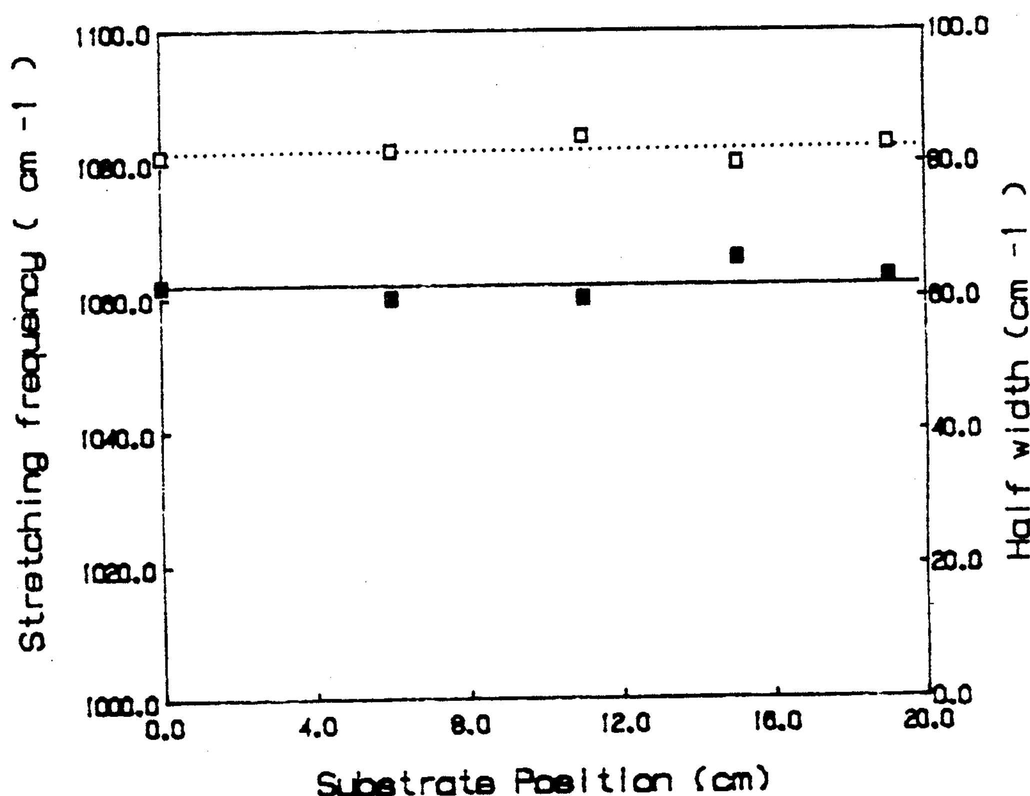

Figure 5.4 γ_m *and* Δ_m *versus substrate position.*

The change in the IR spectra of the heat treated film in a N_2 atmosphere is shown in Fig 5.6. For the as-deposited film, the IR absorption peak position γ_m which was located at 1060 cm^{-1} is

shifted towards higher wave-numbers, similar to thermal oxide film grown at 1000°C which have a peak position γ_m of about 1080 cm^{-1}. The shift in peak position was accompanied by a reduction in the half width. We noticed that the peak does not shift further with longer heating time. This may indicate the composition of the film was entirely SiO_2. The integrated intensity of the 1060 cm^{-1} band as determined by the area under the absorption band increased about 5% consistent with the 5% thickness reduction, indicating that there is no loss of material during heat treatment. Figure 5.7 shows the ratio of thickness d_2/d_1 where d_1 is as-deposited film thickness and d_2 is thickness of the film after heat treatment.

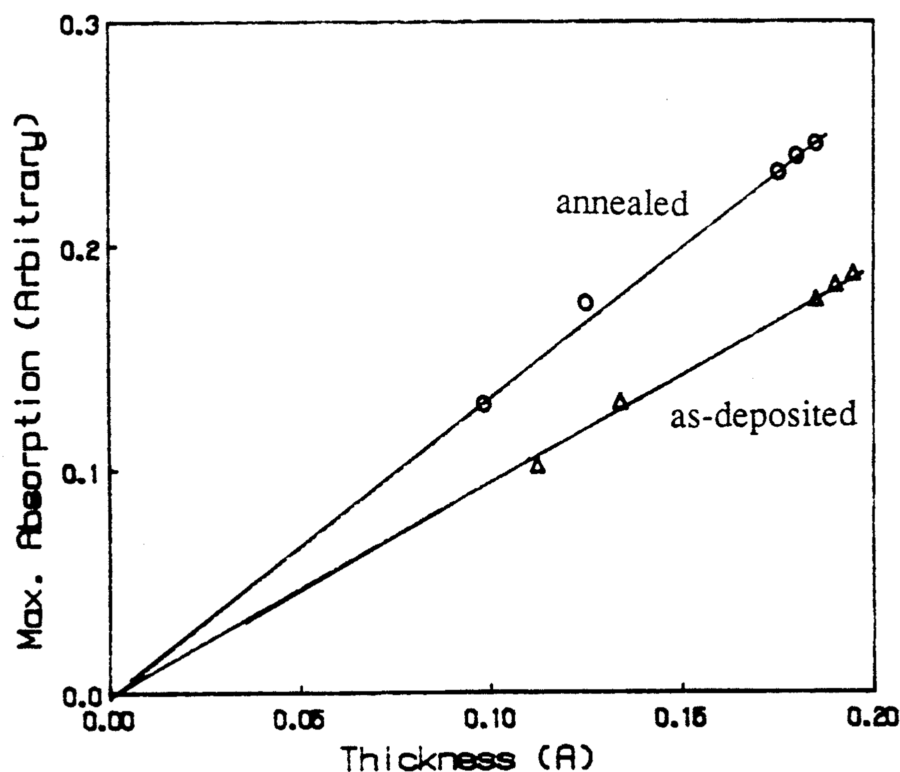

Figure 5.5 *Film absorbance versus thickness.*

The absorbance of 1080 cm^{-1} absorption band after heat treatment is also plotted as a function of film thickness in Fig 5.5 (as indicated by circles). Again, Lambert's law is obeyed. From the slope of each plot, an apparent absorption coefficient defined by $\alpha_{app} = 2.303$ (da/dt) is calculated, where a and t are the band maximum absorbance and film thickness respectively. For films which are heat treated at 1000° C, the value of α_{app} at 1080 cm^{-1} is estimated to be approximately about 3.3×10^4 cm^{-1} in good agreement to $3.2\times10^4 cm^{-1}$ of thermal oxide [8].

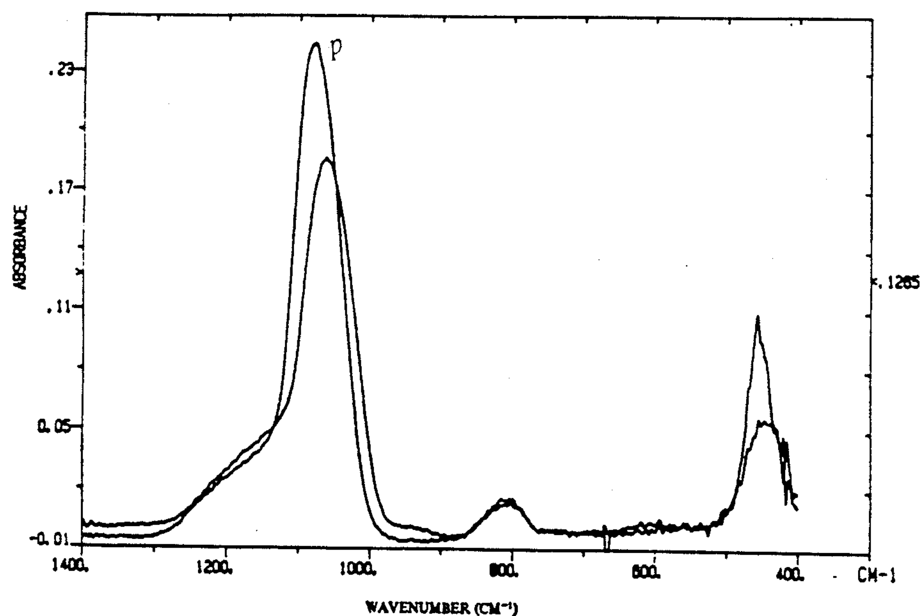

Figure 5.6 *Change of IR spectrum after annealing, p for film after annealing.*

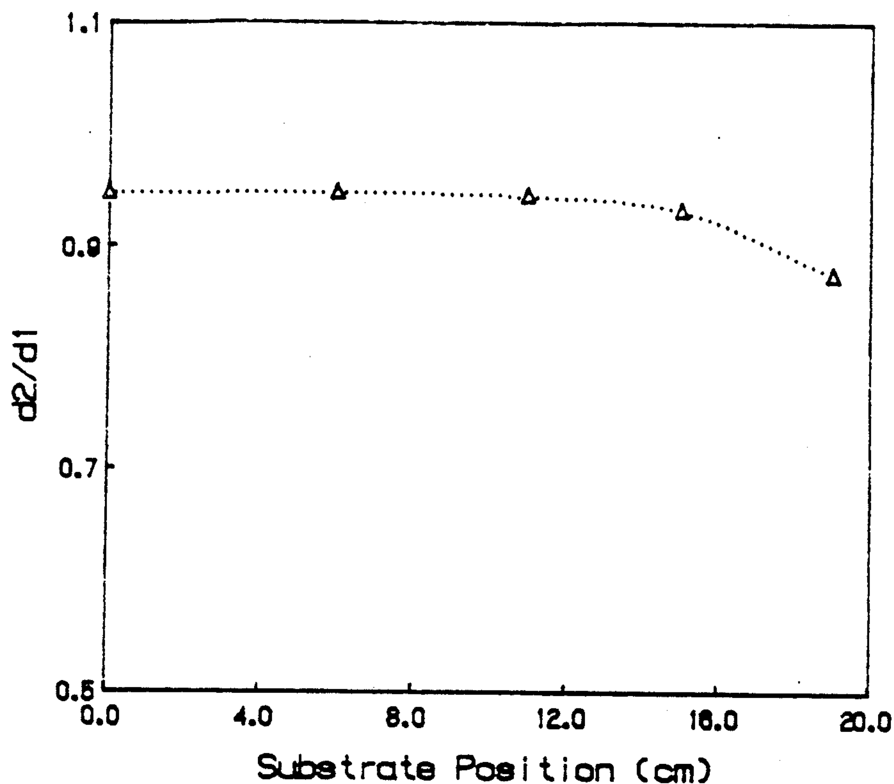

Figure 5.7 *Change in the film thickness after annealing.*

5.2.3 Thickness and Etch Rate.

The ratio of the change in film thickness (d_2/d_1) was also plotted against substrate position as shown in Fig 5.7. According to this graph, films in region 0 - 16 cm have about 5% thickness change. The maximum film thickness deformation was 15% for the substrate 19 cm away from the plasma. This suggests that these films are not as dense as the others. This result also agrees with the films refractive indices as measured by ellipsometry which gave n = 1.384 for films 19 cm away as compared with 1.461 of films deposited at positions of 11 - 15 cm. Film thickness change is believed to be due to film densification alone. We also noted that the results for films at all positions have refractive

indices slightly lower than films deposited at the same position but with substrate surface normal to magnetic field lines. The reason for this may be explained as following, the films grown in positions normal to magnetic field line are still under mild ion or electron bombardment, while on other hand, magnetic screening has prevented the bombardment of the growing films in positions parallel to the magnetic field lines [12]

Figure 5.8 shows the wet etching rate of the as-deposited films in a P-etch solution. The films exhibited fast etching rates at both the near and far substrate positions as compared to the films grown in the middle position. The result is in well agreement with the thickness deformation of films grown 19 cm away from the plasma (ie. the fast etching rate due to the less dense film). However films grown in region 0 - 8 cm behave differently, although there is only a 5% thickness change after annealing they have very high etch rates. The explanation for this may due to the substrate being emerged inside plasma with heavy gas phase reactions taking place during film deposition. The result is a very porous film as evidenced by the surface roughness detected by ellipsometry.

Figure 5.8 also shows the etch rate of films after heat treatment. All the films considered have their etch rate reduced between a factor 5 - 6 Å/sec. Films grown in region 10 - 16 cm show very good etching rates comparable to results reported on PECVD SiO_2 using an rf system after heat treatment. This result again confirms damage of films in the region between 0 - 8 cm which the 1000^oC annealing still gives relative high etch rate.

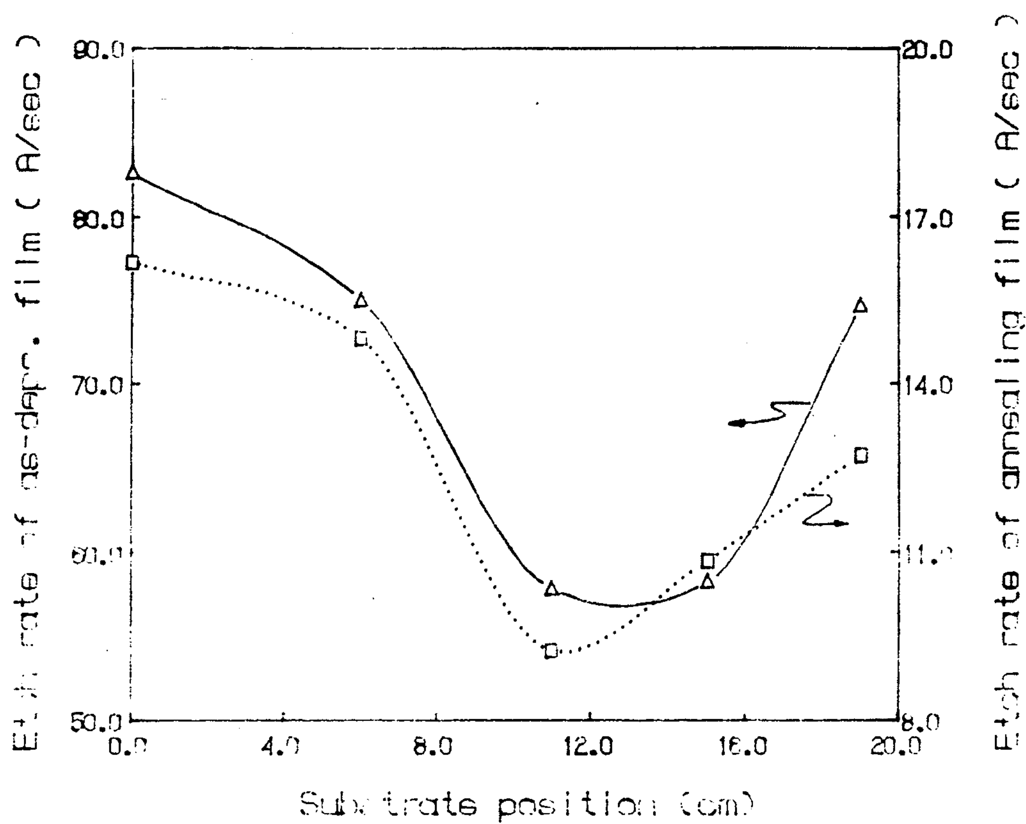

Figure 5.8 *Etching rate of as-deposited and annealing films as functions of substrate position.*

5.3 Conclusions.

In conclusion, films deposited in direct contact with the plasma are mainly a result of gas phase reactions and heavy interaction with all plasma radicals. Films are porous and have fast etch rates even after high temperature annealing. Films deposited too far away from the plasma are not dense either, hence film formation may due to mainly neutral species. Film structure may be a more random distribution of Si-O bonding which are easily densified by subsequent heat treatment. Films grown at a distance 10-16 cm away from the plasma have better quality than the films grown at both ends. These films may be of higher quality if a moderate degree of ion bombardment enhances surface reactions.

5.4 Future Trends.

Damage free SiO_2 films cannot be avoided when grown directly in the plasma of PECVD systems. Even though down stream processes can be used to deposit SiO_2, we may encounter problems associated with film densification and the higher cost of the plasma generating system. Another method of growing insulating films recently initiated is called photochemical CVD[10]. Photochemical CVD is a much simpler process without generating energetic species that may damage the film, it also is less expensive to built than any PECVD system and looks like a promising method of the future.

5.5 References for Chapter 5.

1 G. Lucovsky, S.Y. Lin, P.D. Richard, S.S. Chao, Y. Takagi, P. Pai, J.E. Keem, and J.E. Tyler, J. Non-Cryst. Solid 75, 1985, pp. 429-434.

2 P.G. Pai, S.S. Chao, Y. Takagi, G. Lucovsky, J. Vac. Aci. Tech. A 4(3), 1986, pp. 689-694.

3 J. Batey and E. Tierney, J. Appl. Phys. 60 (9), 1986, pp. 3136-3145.

4 T.V. Herak, T.T. Chau, D.J. Thomson, S.R. Mejia, D.A. Buchanan, R.D. Mcleod, and K.C. Kao, to be published in the proceeding of the America Physical Society, 1988.

5 L.G. Meiners, J. Vac. Sci. Technology, 21 (2), 1982, pp. 655-658.

6 S.R. Mejia, R.D. McLeod, K.C. Kao, H.C. Card, Rev. Sci. Intrum. 57, 1986, pp. 493-496.

7 G. Lucovsky, M.J. Manitini, J.K. Sirivastava, and E.A. Irene, J. Vac. Sci. Technology, B5 (2), 1987, pp - 530-537.

8 I.W. Boyd and J.I.B. Wilson, J. Appl. Phys. 53(6), 1982, pp. 4166-4172.

9 K. Inoue, M. Michimori, M. Okuyama, and Y. Hamakawa, Jpn. J. Appl. Phys. 20 (6), 1987, pp. 805-811.

10 Y. Toyoda, K. Inoue, M. Okuyyama, and Y. Hamakawa, Jpn. J. Appl. Phys. 26 (6), 1987, pp. 835-840.

11 B. Robison, P.D. Hoh, P. Madakson, T.N. Nguyen, S.A. Shivashankar, IBM T.J. Watson Research Center, Yorktown

Heights, New York 10598, 1987.

12 S.R. Mejia, T.T. Chau, R.D. McLeod, K.C. Kao, H.C. Card, to be published in the Canadian Journal of Physics.

CHAPTER 6

Conclusions.

Even though conclusions have been provided separately for each chapter. This chapter will briefly conclude some of the main issues of the whole thesis.

In chapter 1, we presented a brief look at some chemical aspect of gas reactions inside a plasma. Plasma processing for such as etching and thin film deposition were given as examples to give us a basic understanding of plasma processing mechanisms.

In chapter 2, we presented a review of ECR microwave systems. several different system configurations were described. The application areas are also mentioned.

In chapter 3, we presented an experimental work on the dry etching process. We concluded that in microwave ECR plasma enhance chemical etching, atomic fluorine is the main species in the etching mechanism playing a comparable role as that found in rf systems. However, since in an ECR system, the operating pressure is much lower than in rf systems, we anticipate that anisotropic etching can be obtained with reduced substrate damage and we have proposed some directions further research.

In chapter 4, we presented the effect of bias on a-Si:H thin film deposition. We have shown that mild ion bombardment enhances a-Si:H thin film deposition and resulted in good film properties; both optical and electronic.

In chapter 5, we presented a preliminary study of insulating thin film deposition utilizing SiH_4 and O_2 gas discharges. Thus far, films show good trends with respect to the FTIR studies. We

believe that good SiO_2 films can be fabricated by an ECR plasma system without the need for a carrier gas. Future experimental work is required to support this position.

APPENDIX A

In general the Plasma frequency is expressed as :

$$f_p^2 = \frac{N_e \, q^2}{4 \, \pi^2 \, m \, \varepsilon_o}$$

Where N_e electron density, m : electron mass, q : electronic charge, ε_o : permeativity of free space.

Under the external DC magnetic field, the electron cyclotron frequency w_c is

$$w_c = \frac{q \, B}{m}$$

where B is the magnetic field.